Magnetic Force Microscopy of Magnetic Nanoparticles

A Senior Honors Thesis

Presented in Partial Fulfillment of the Requirements for Graduation *with research distinction in Physics* in the undergraduate colleges of The Ohio State University

By

Michael Page

The Ohio State University

December 2010

Project Advisor: Professor Chris Hammel, Department of Physics

Table of Contents

1. Introduction:

The use of magnetic nanoparticles in biology is becoming increasingly important for applications such as biosensors and targeted drug delivery, and as a method for the labeling and sorting of cells[1-3]. In addition, many degenerative diseases, such as Alzheimer's, Huntington's, Parkinson's disease and atherosclerosis, can be characterized by nanoscale Fe(II) and Fe(III) deposits in affected tissue[4-7]. Both the naturally occurring magnetic nanoparticles and those synthetically prepared for use in biological applications are less than 100 nm in size and are typically superparamagnetic or paramagnetic in nature. One of the inherent issues in detecting nanoparticles in this size range is that they often only possess a stable magnetic moment in the presence of an applied magnetic field. It is therefore difficult to image and spatially localize these nanoscale magnetic domains at the subcellular level. Knowledge of the characteristics of the magnetic particles that contribute to its magnetic properties, such as ionic composition and crystal symmetry, can provide information on the biological system in which they occur[8].

In order to understand the particle size and magnetic nature of these nanoparticles, a specialized technique which combines high spatial resolution with optimal force sensitivity is required. For this thesis project, magnetic force microscopy (MFM), a scanned force microscopy based technique, was used to detect and localize magnetic nanoparticles. MFM utilizes a magnetic probe, a nanoscale ferromagnetic structure which interacts with a localized volume of sample magnetization, which is brought close to the sample and interacts with the magnetic

field gradients near the surface. MFM detects local magnetic interaction by measuring deflections of the tip due to tip–sample magnetic interaction as it scans across the sample. MFM has been previously used as a technique to localize and characterize macroscale magnetic domains in materials and more recently for larger magnetic nanoparticles[9,10]. However, the ability of MFM to detect a signal from nanoscale magnetic particles is still in question[11]. There have been some reports on the possible uses of MFM for detection of such particles occurring naturally in biological systems. These include detection of iron compounds in neurological disorders[12], magnetic domains in magnetotactic bacteria[13], and iron deposits in Hepatitis B-diseased livers[14]. Limited studies exist on localizing and detecting magnetic nanoparticles in vitro[15,16] or in cell-based systems[17]. A systematic and quantitative study of the applicability of MFM for characterizing magnetic nanoparticles in ambient air is lacking. The goal of this project is to obtain and analyze magnetic force microscopy images from such nanoparticles.

2.1 Background: Principles of Magnetic Force Microscopy

1: Principles of Operation

Magnetic Force Microcopy(MFM) utilizes a flexible lever, called a cantilever, with a magnetic tip to map force gradients near the surface of a sample. A typical cantilever is around 200 μm long by 30 μm wide and 3 μm thick. The force on the cantilever is determined by optically measuring the displacement of the end of the cantilever. For a typical MFM application, the forces on the cantilever are on the order of pico-newtons with cantilever deflections on the scale of nanometers. This deflection can be measured using soft Silicon cantilevers with spring constant of .01 to 1 $\frac{N}{m}$. The mathematical arguments that follow were adapted from *Principle of Magnetic Force Microscopy* by Leon Ablemann[18].

The force F exerted by the stray field on the cantilever tip causes the tip to deflect either toward or away from the sample surface by a distance Δz

$$\Delta z = \frac{F_x}{k} \tag{1}$$

where k is the cantilever spring constant. For small deflections, the cantilever can be treated as a damped harmonic oscillator with spring constant k, mass m, and damping constant γ. When an external oscillating force

$$F_z = F_o \cos(\omega t) \tag{2}$$

is applied to the cantilever, the resulting displacement is also harmonic, but has a phase shift for

$$\omega > 0 \Rightarrow F_z = F_o \cos(\omega t + \phi(\omega)) \tag{3}$$

This force is applied to the end of the cantilever by using a piezoelectric stack mounted to the holder.

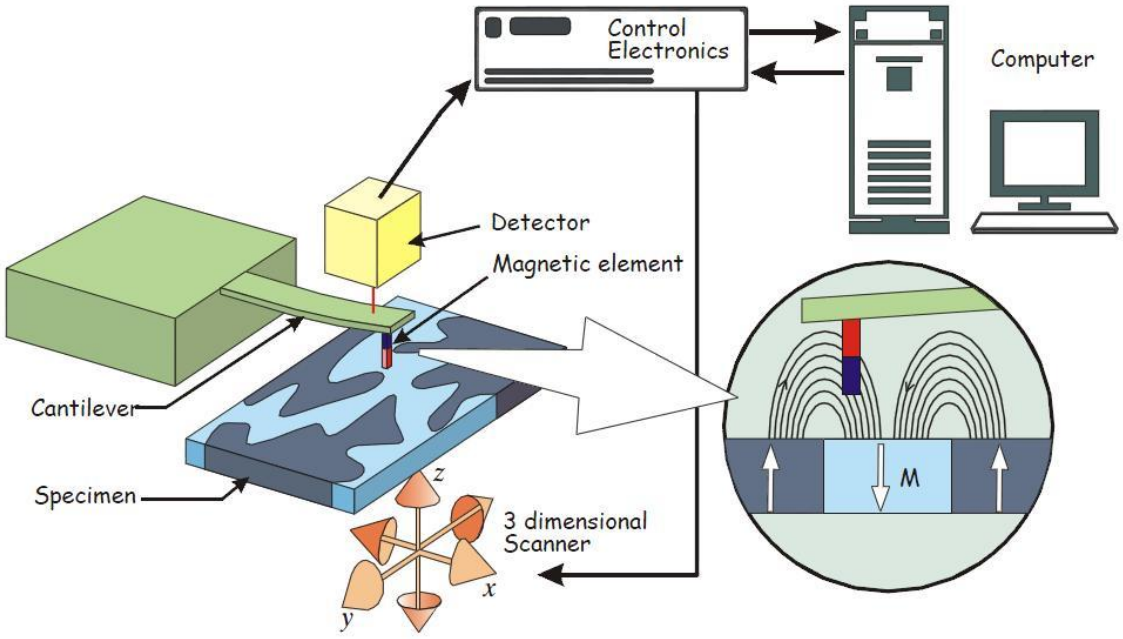

Figure 1: Schematic of Atomic Force Microscope[19].

For the mathematical discussion of the displacement of the cantilever, we will work in the Laplace domain where

$$\hat{F}(s) = \int_{-\infty}^{\infty} f(t)e^{-st}dt \tag{4}$$

In the Laplace domain, the ratio of the displacement to force is

$$\frac{\hat{Z}}{\hat{F}} = \frac{1}{k + s\gamma + ms^2} \tag{5}$$

If we use the resonance frequency ω_o and unitless damping factor δ

$$\omega_o = \sqrt{\frac{k}{m}}, \quad \delta = \frac{\gamma}{2\sqrt{mk}} = \frac{\gamma\omega_o}{2k} \tag{6}$$

We can write (5) as

$$\frac{\hat{Z}}{\hat{F}} = \frac{1}{m\omega_o^2 + 2\delta\omega_o ms + ms^2} \tag{7}$$

In the field of scanned probe microscopy one usually discusses the quality factor, Q, of resonance. The quality factor is the ratio of energy stored in the cantilever to the energy lost per cycle:

$$Q = 2\pi \frac{Energy\ stored\ in\ cantilever}{Energy\ lost\ per\ cycle} = 2\pi\ \frac{\frac{1}{2}k{z_o}^2}{\pi\gamma{z_o}^2\omega_o} = \frac{k}{\gamma\omega_o} = \frac{1}{2\delta} \tag{8}$$

Rewriting (7) with Q gives:

$$\frac{\hat{Z}}{\hat{F}} = \frac{1}{m\omega_o^2 + \frac{\omega_0 m}{Q}s + ms^2} \tag{9}$$

From (9) we can calculate the amplitude z_o of the cantilever when driven at a frequency ω

$$z_o = \frac{{F_o}/{m}}{\sqrt{(\omega_o^2 - \omega^2)^2 + (\omega_o\omega/Q)^2}} \tag{10}$$

And the phase shift ϕ between the force and the deflection is

$$\phi = tan^{-1}\left(\frac{\omega_o\omega}{Q(\omega_o^2 - \omega^2)}\right) \tag{11}$$

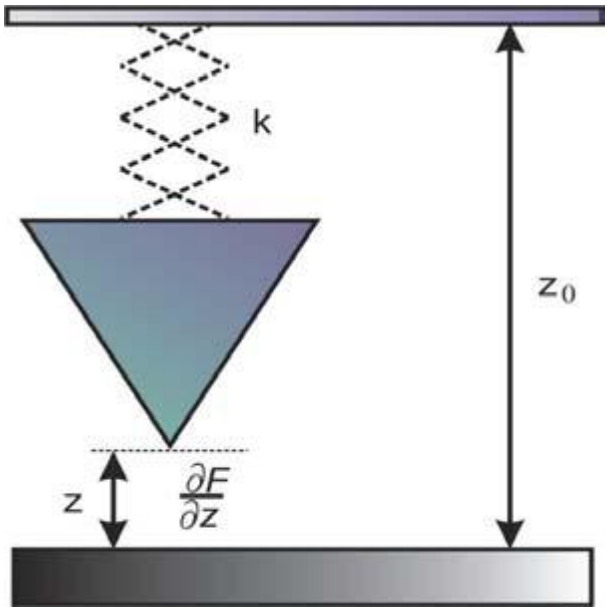

Figure 2 Modeled tip-sample interaction, where k denotes cantilever constant and the force derivative $^{\partial F}/_{\partial z}$ is schematically depicted here as an additive force interaction constant[20].

The force on the magnetic tip increases as it approaches the sample. The tip can be thought of as having its own internal spring constant and a second spring constant as if there is another spring attached to the cantilever. The second spring has a spring constant $^{\partial F}/_{\partial z}$ and is a result of the force acting on the cantilever. If the cantilever deflection is small enough so that $^{\partial F}/_{\partial z}$ can be considered a constant, this result in a change of the resonance frequency of $f_{o} = {}^{\omega_o}/_{2\pi}$ of the cantilever.

$$f_0' = f_o\sqrt{1 - \frac{{}^{\partial F}/_{\partial z}}{k}} \tag{12}$$

$$\Delta f = f_0' - f_o \approx -\frac{f_0}{2k}\frac{\partial F_z}{\partial z} \tag{13}$$

The above approximation is valid when the change in the cantilever frequency is much smaller than the cantilever's resonance frequency, which is usually the case in MFM. The sign of the change in frequency needs to be noted. Since the above equations assume that the positive z direction is pointing away from

the sample, when the tip is attracted towards the sample, the force is negative and the force derivative is positive. Therefore, for attractive forces, the resonance frequency of the cantilever decreases, and for repulsive forces the resonance frequency of the cantilever increases.

There are two ways to determine the change in frequency of the interacting cantilever. The first is amplitude detection. In amplitude detection, the cantilever is oscillated at a fixed frequency slightly off resonance. Tip-sample interactions cause changes in this frequency which results in changes in the cantilever's oscillation amplitude. These changes in the oscillation amplitude can then be used to determine the interacting tips new frequency referred to as f_o' above. In the second detection mode, called 'phase detection', the frequency of the driving signal is fixed to the resonance frequency. When the tip interacts with the sample, there is a change of phase of the oscillation. The phase difference between the driving signal and the measured cantilever deflection is used to determine the interacting tips new frequency, f_o'. The changes in the frequency, whether measured by 'amplitude detection' or 'phase detection,' can then be used to determine the force interacting with the cantilever as shown in equation 13 above.

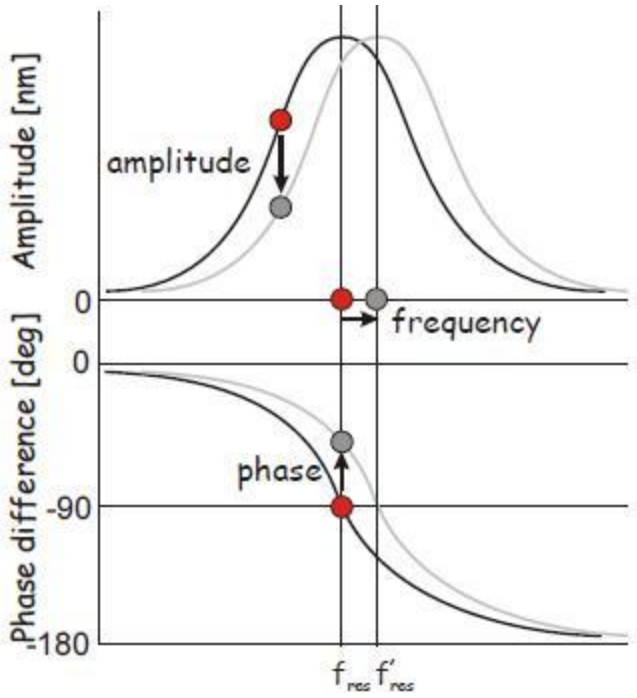

Figure 3: A change of the magnetic force on the tip results in a change in resonance frequency of the cantilever, which can be detected in two ways[21.]

When operating in the MFM mode, the crucial issue is distinguish between the surface topography of the sample and the magnetic signal. To solve this problem, MFM measurements are performed by scanning the same line twice or what is referred to as a two pass mode.

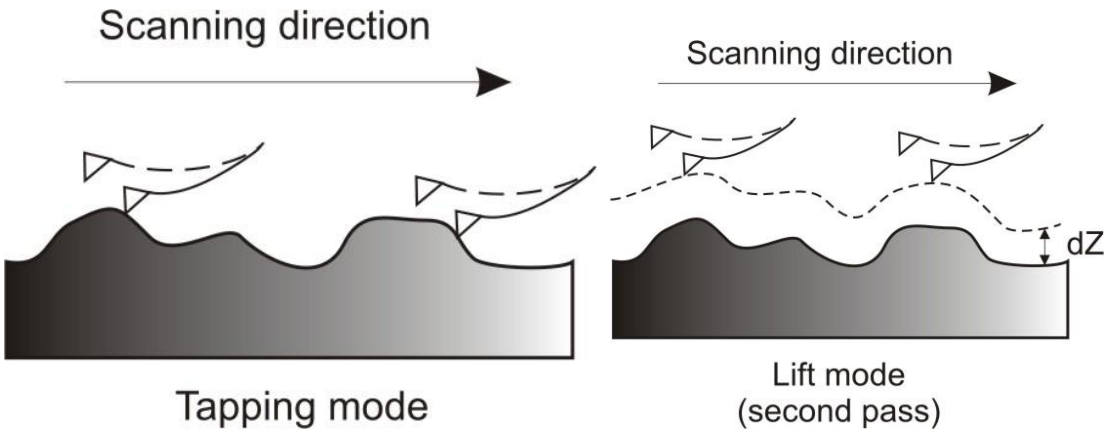

Figure 4: Two pass scanning method for MFM [22].

In the two pass mode, the first scan or pass uses the semi-contact (tapping) mode of operation, where the surface topography is recorded to be used in the second scan (Fig.4). After the first scan, the cantilever is lifted above the surface at required height *dZ* and follows the same topographic contour. Because of the height *dZ*, the cantilever is only affected by long-ranged magnetic forces.

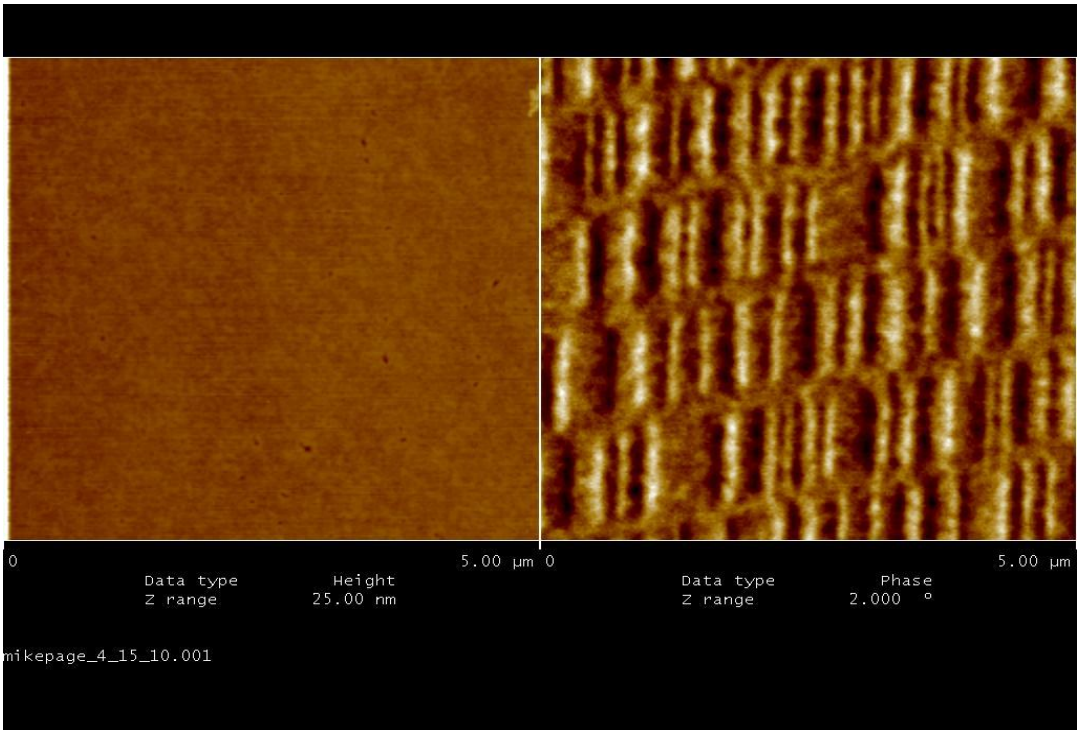

Figure 5: Left Image is first pass: surface topography imaging-tapping mode (hard drive). Right Image is second pass: lift scan follows the topography to obtain magnetic image (hard drive).

2: Magnetic Interaction

In order to calculate the force gradient on the magnetic tip, we first need to determine the energy U of the tip/sample system. Once the energy is determined, we can get the force by taking the gradient of the energy. The energy can be calculated by either treating the magnetic tip as interacting with the stray field of the sample or by treating the magnetic sample as interacting with the stray field of the tip. The more convenient choice depends on the specific problem. If we follow the first case and treat the tip as a magnetized element interacting with the stray field of the sample, the magnetic energy is:

$$U = -\mu_o \int_{tip} \vec{M}_{tip} \vec{H}_{sample} \, dV_{tip} \tag{14}$$

where μ_o is the vacuum magnetic permeability, $\vec{M}_{tip}$ is the magnetization of the tip, and $\vec{H}_{sample}$ is the stray field of the sample. The force is therefore:

$$\vec{F} = -\nabla U = -\mu_o \int_{tip} \nabla \vec{M}_{tip} \vec{H}_{sample} \, dV_{tip} \tag{15}$$

This equation can be simplified to the familiar form:

$$\vec{F} = -\left(\vec{m} \cdot \vec{\nabla}\right)\vec{H} \tag{16}$$

Once the force is determined, we can take the gradient of this force to determine the interaction between the tip and the sample. Our long-term goal is to use this theory to perform a quantitative analysis of the MFM data I obtained while working on this project.

2.2 Magnetic Properties of Nanoparticles

Biological systems can contain a wide range of magnetic particles and it is important to note that a nanoparticle's magnetic properties are greatly dependent on its size. These particles can be smaller than 35 nm, in which case they are often superparamagnetic, or they can be much larger, around 100 nm and up to 600 nm, and can be paramagnetic or ferromagnetic[23-25]. The naturally occurring magnetic particles in mammalian tissue often consist of a mixture of ferromagnetic, superparamagnetic, and paramagnetic particles.

While many of the mechanisms and properties of magnetic nanoparticles are not fully understood, there are general trends which we can make use of when attempting to image such particles. The first trend is the switch from ferromagnetism to superparamagnetism. As the particle size decreases, nanoparticles have insufficient volume for a stable magnetic moment. The thermal energy allows for spontaneous reversal of the magnetization, making these particles 'superparamagnetic'. If the magnetic nanoparticles are superparamagnetic, they only posses a stable magnetic moment in the presence of an applied external magnetic field. Therefore, a method of applying an external magnetic field in conjunction with MFM was needed to make my project a success.

The second trend is that the saturation magnetization of nano-sized magnetic materials is smaller than that of their bulk counterparts. This increases the difficulty of obtaining an MFM image of magnetic nanoparticles. Therefore, in order to image the particles, the sample tip separation must be small enough to detect these forces. However, the cantilever is not force selective. The force the cantilever feels is the sum of all such forces acting on the cantilever.

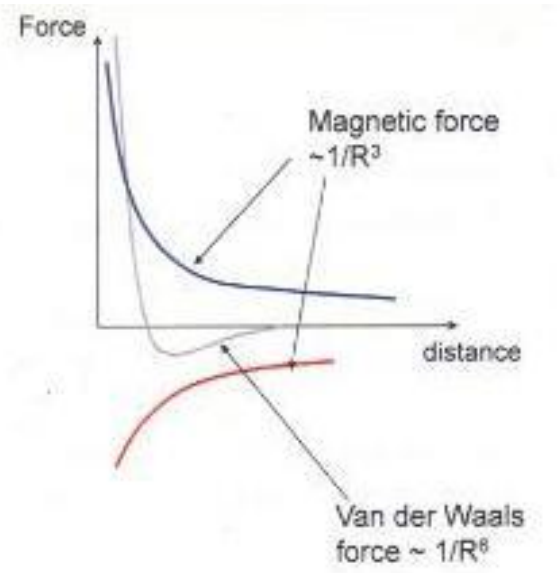

Figure 6: Plot of magnetic and van der waals forces.

In order to distinguish magnetic signals from surface feature, or Van der Waals signals, the cantilever is usually raised away from the surface so that the longer ranged magnetic force dominates. However, to compensate for the weak magnetic interactions resulting from the smaller magnetization of these superparamagnetic nanoparticles, the tip must be brought near the sample surface. This creates a convolution of the magnetic and surface feature forces acting on the tip. Since we desire to map only the magnetic signal of these particles, I needed to develop a convenient way to 'filter out' surface topography signal from the Van der Waals interaction. The best way to accomplish this is to apply a variable external magnetic field to the nanoparticles and observe the contrast in the MFM signal upon switching the applied field. For this project to be successful, I needed to develop a device that could both apply an external field to stabilize the moment of the nanoparticles as well as switch the field in order to create a changing magnetic signal that could be separated from the surface topography. The design and implementation of this device is described in the next section.

3. Magnetic Field Stage Construction

The magnetic field stage must be able to apply a variable external magnetic field of sufficient strength to reverse the magnetization of the nanoparticles and work in conjunction with the atomic force microscope that is available to us. In order to easily vary the magnetic field, electromagnets will be used so that the direction of the field can be reversed by reversing the applied current. The electromagnets need to produce a field of at least 100G at the location of the sample of in order to reverse the magnetization of the nanoparticles. In order to ensure the proper field strength, the relation between the size of the electromagnet and the distance from the sample must be determined. The on axis field produced by a finite solenoid is given by:

$$B_z = \frac{\mu_o NI}{2}[cos\theta_1 - cos\theta_2] \quad (17)$$

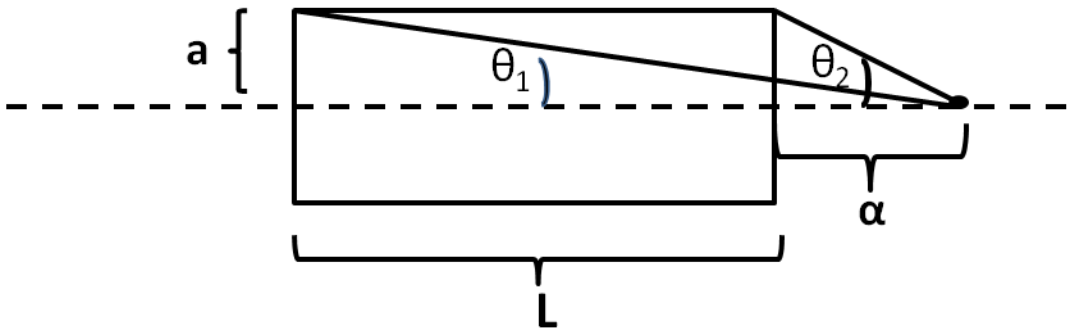

Figure 7: Representation of a solenoid for the calculation of the on axis magnetic field.

where μ_o is the magnetic permeability of the vacuum, I is the current, N is the number of turns per unit length, and the angles are as defined in figure 7. Rather than building our own electromagnets, we chose to purchase electromagnets from a manufacturer called Magnetech. The electromagnets purchased are cylindrical and 1.25" in diameter by 1.25" in length.

Figure 8: Left, Magnetech electromagnets. Right, Keithley 2425 current source.

We used a Keithley 2425 current supply to power the electromagnets which can accept up to three Amps of current. The magnetic field was measured using a gauss meter and the electromagnets produce a field of 130 G 3/8’ away from the magnet face at 1.0 A current. In order to ensure that the electromagnets magnetization is reversed when the current is reversed, the field vs. current was measured to determine the hysteresis of the electromagnets. The field was measured by using a hand held gauss meter. While the fields measured here are accurate relative to each other, the actual fields measured are highly dependent on the exact position and orientation of the hall probe. Therefore, the actual magnetic fields produced by the electromagnet are measured to an accuracy of a few gauss as this is the change in the measured field resulting from moving the hall probe by a small amount.

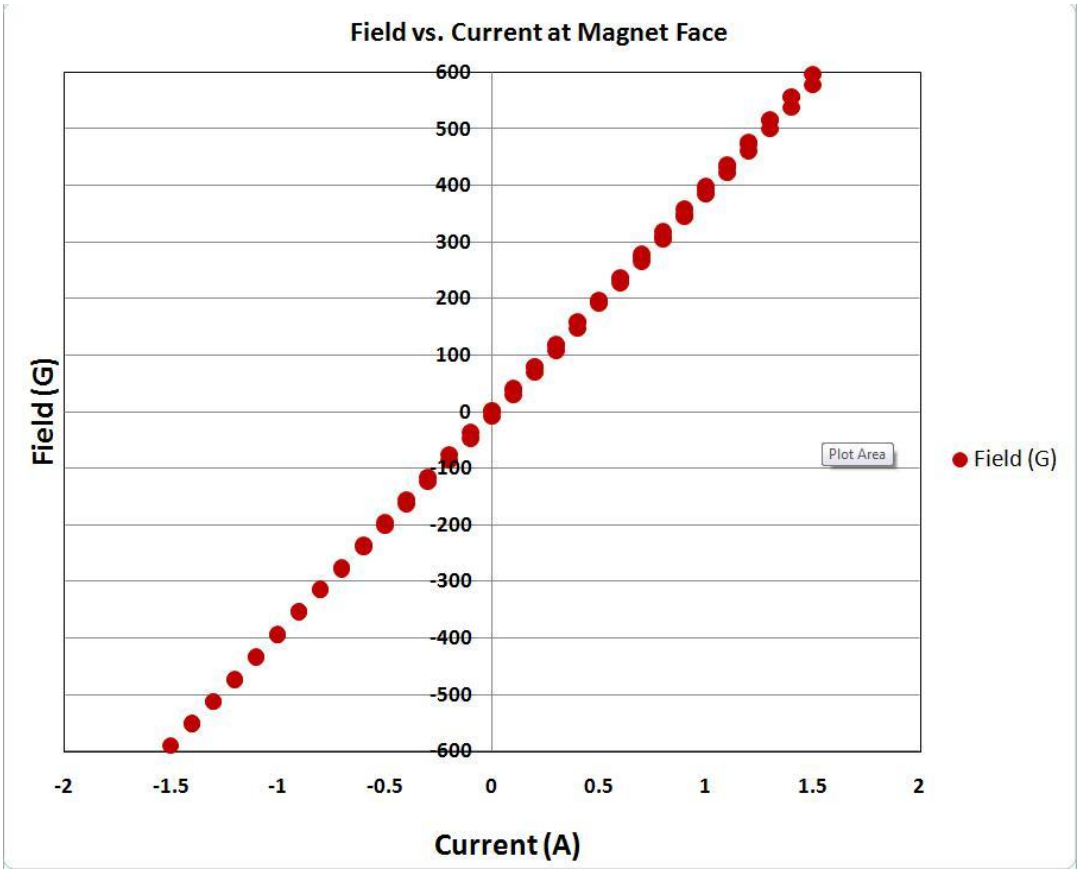

Figure 9:Magnetch electromagnet hysteresis measurement.

In order to use the electromagnets in conjunction with MFM, I needed to construct a stage that could be attached to the facility commercial atomic force microscope, pictured in figure 10. . The stage must be designed to work within the restraints of the Veeco Dimension 3000 AFM. The chief constraint is that the electromagnets must fit in around the scan head of the microscope.

Figure 10: Veeco Dimension 3000 atomic force microscope

The stage design needs to allow the magnets to be moved close to the sample and the stage should be attached to the motorized plate of the AFM microscope so that it can be positioned with the controls already present in the microscope software. The chief problem with this design is the limited height to which the scan head can be raised so that the new stage can fit under the scan head while positioning the sample a close as possible to the central axis of the electromagnet. It is desirable for the sample to be on the axis of the electromagnet for the maximum field and in order simplify any calculations. The stage that I designed to fit these requirements is shown in figures 11 and 12 below. I used Autodesk inventor, a 3D autocad software, to design the stage which was then fabricated by the OSU Machine Shop. The drawing and finished product are shown below.

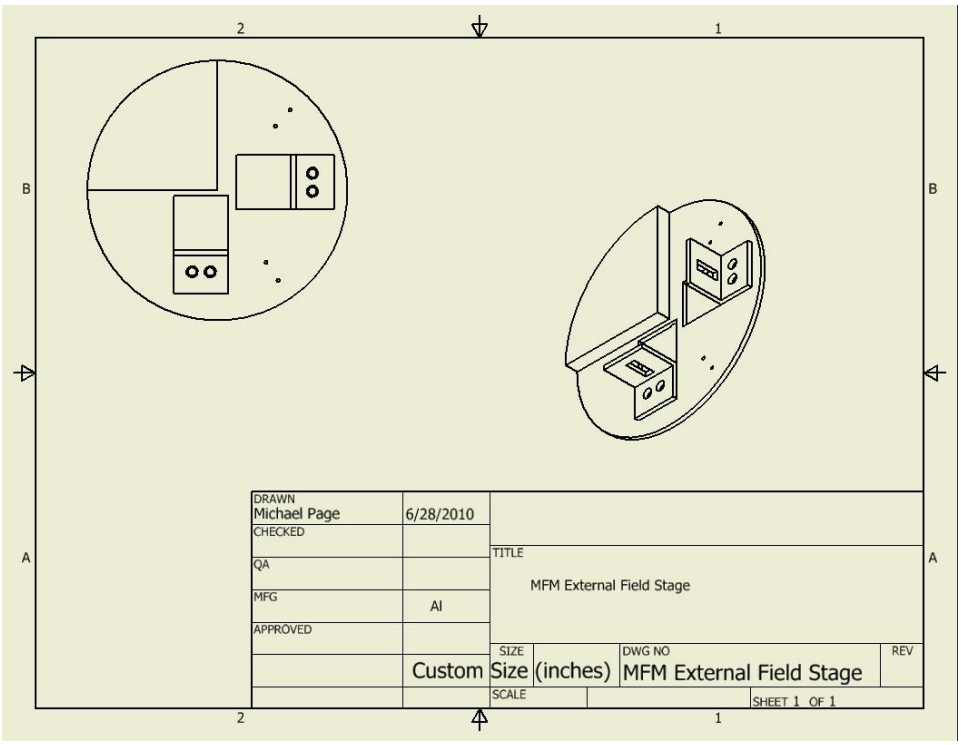

Figure 11: Autodesk Inventor drawing of external field stage

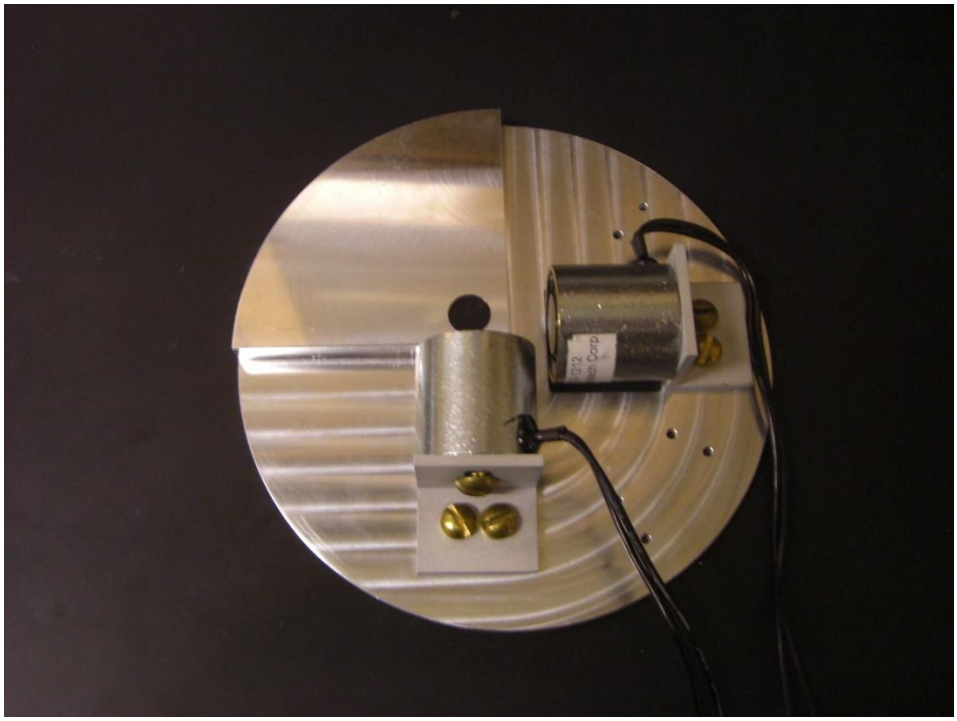

Figure 12: Fabricated stage for applying external magnetic fields in conjunction with MFM

The stage is designed so that both of the magnets can be positioned as close as possible to the sample while still fitting around the scan head. One of the magnets is further away from the sample location than the other to allow for the cantilever holder which protrudes from the scan head in that direction. The distances between the sample and the electromagnets are 3/8” for the closer electromagnet and 3/4'” for the farther electromagnet. Therefore, the fields measured at these distances are the fields which the sample will be exposed to during an experiment and are shown in the table below.

Current (A)	Field at Face (G)	Field at 3/8 ‘’ (G)	Field at ¾ ‘’ (G)
Positive .72	275	90	30
Positive 1.0	400	130	45
Positive 1.5	570	200	80

Figure 13: Magnetic field produced by electromagnets at measured gaps and currents.

4. Nanoparticle Characterization

While the ultimate goal is to perform quantitative MFM of sub 100 nm particles, the difficulty in obtaining any MFM image from such particles cannot be understated due to their unstable magnetic moments requiring a stabilizing field and their small magnetic forces requiring small tip-sample separations and therefore magnetic and surface feature force convolutions. Therefore, I decided to image nanoparticles of a larger size in order to test my imaging technique and familiarize myself with the problems I might encounter with the more difficult system.

I imaged Iron-Cobalt nanoparticles that were fabricated by Michael McHenry at Carnegie Mellon University. These nanoparticles are created by a radio frequency plasma torch and the sample is purported to consist of particles with radii ranging from 100 nm to 700 nm. The particles are initially in a powder form and must be dispersed onto a substrate for imaging. In order to disperse the nanoparticles, I first diluted them in chloroform and then deposited a drop of the solution onto a clean silicon wafer. I allowed the chloroform to evaporate naturally, leaving behind the dispersed particles. I chose chloroform despite its hazardous nature because it evaporates very cleanly. Other solvents, such as hexane or ethanol, leave behind a residue as they evaporate which makes it difficult to locate and obtain magnetic signals from the nanoparticles.

The results from this dispersion method were unsatisfactory. While the nanoparticles are in powdered form, the particles stick together and result in large agglomerations which prevent the imaging of separated nanoparticles. Images of such agglomerations are shown below.

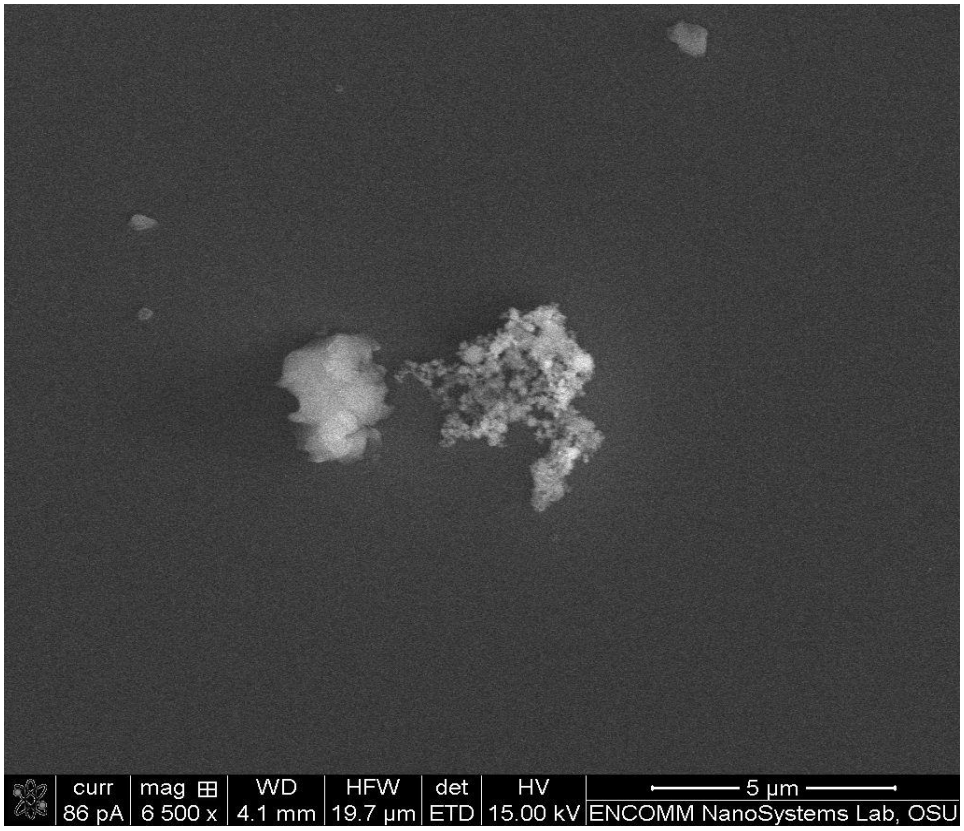

Figure 14: Scanning electron microscopy image of FeCo nanoparticle super lattices. These particles were dissolved in chloroform, deposited on a Si substrate, and allowed to evaporate naturally.

In order to image the magnetic signal from a single nanoparticle, they must be dispersed uniformly on the silicon wafer. Therefore, an improved method of nanoparticle dispersion was needed. I decided to try a technique of "washing" the particles in isopropanol and centrifuging them before dispersion, which I learned from our collaborator in bio-medical engineering. The exact dispersion procedure is shown below.

- 1. Place 10mg of the dry FeCo particles into a clean, dry, glass vial.
- 2. Add 6 ml of chloroform
- 3. Use a vortex mixer to put the particles into solution.

- 4. Place 1mL of FeCo/solvent solution from step 3 into a clean, dry, **glass** test tube and add 2mL of isopropanol.
- 5. Centrifuge the tube at 3500 rpm for 3 minutes.
- 6. Pour off the supernatant solvent, leaving the particles at the bottom of the test tube
- 7. Add 2mL of isopropanol solvent into test tube, use a pipette to mix the particles into the solvent.
- 8. Centrifuge the tube again at 3500rpm for 3 minutes.
- 9. Pour off the supernatant solvent, leaving the particles at the bottom of the test tube
- 10. Add 2mL of chloroform solvent into test tube, and use a pipette to mix particles into solution.
- 11. Use this solution to prepare samples.

This method of nanoparticle dispersion produced excellent results. The nanoparticles were uniformly dispersed. Images of the dispersion are shown below.

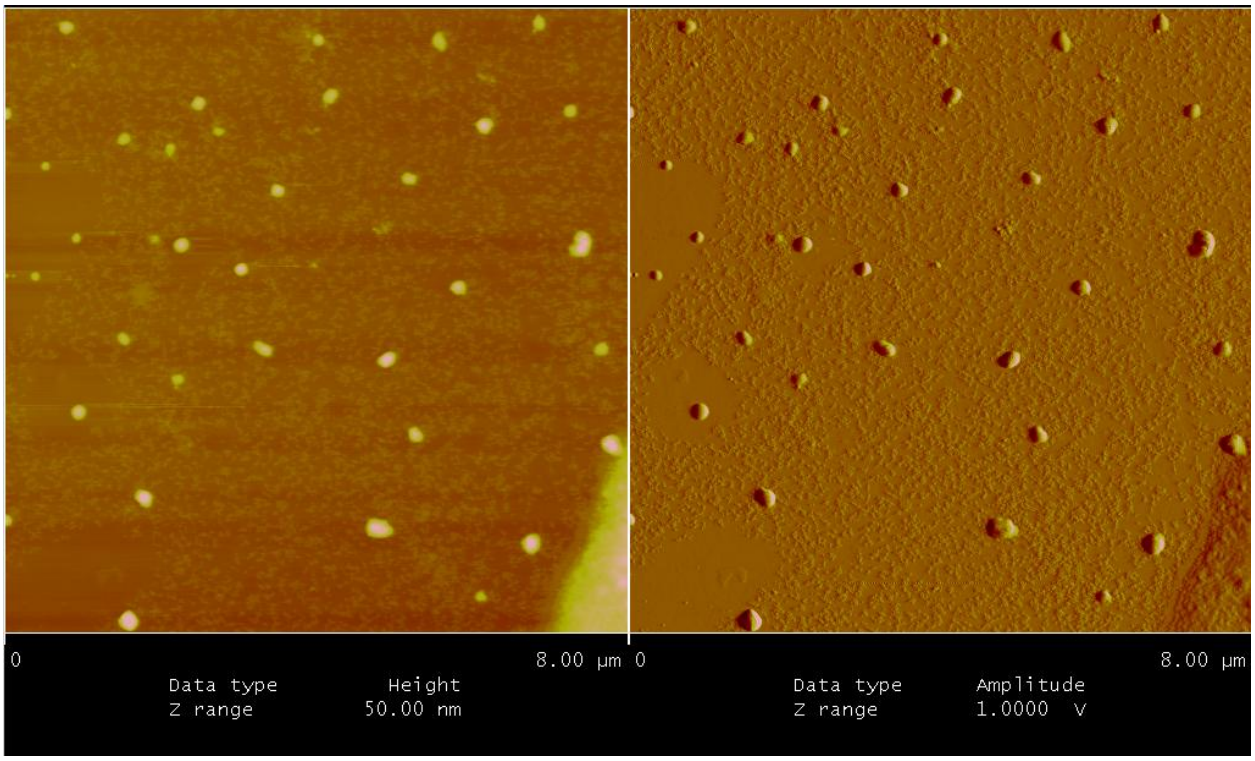

Figures 15: Left side, AFM height measurements of FeCo nanoparticles dispersed on silicon. Right side, AFM amplitude error measurements of FeCo nanoparticles dispersed on silicon.

The Nanoparticles shown in the previous two images have an average radius of 100 to 200 nm. The nanoparticles that we image for the remainder of the project and which will be discussed below are also close to this size range, with the majority being around 100 nm.

To ensure that we were imaging the particles and not some dirt or solvent residue, we also imaged the nanoparticles with energy dispersive x-ray spectroscopy (EDX). Because it is difficult to get an EDX signal from an individual nanoparticle because their small size allows electrons to penetrate them, we chose to confirm the elemental composition of the nanoparticles by performing EDX on the larger aggregates.

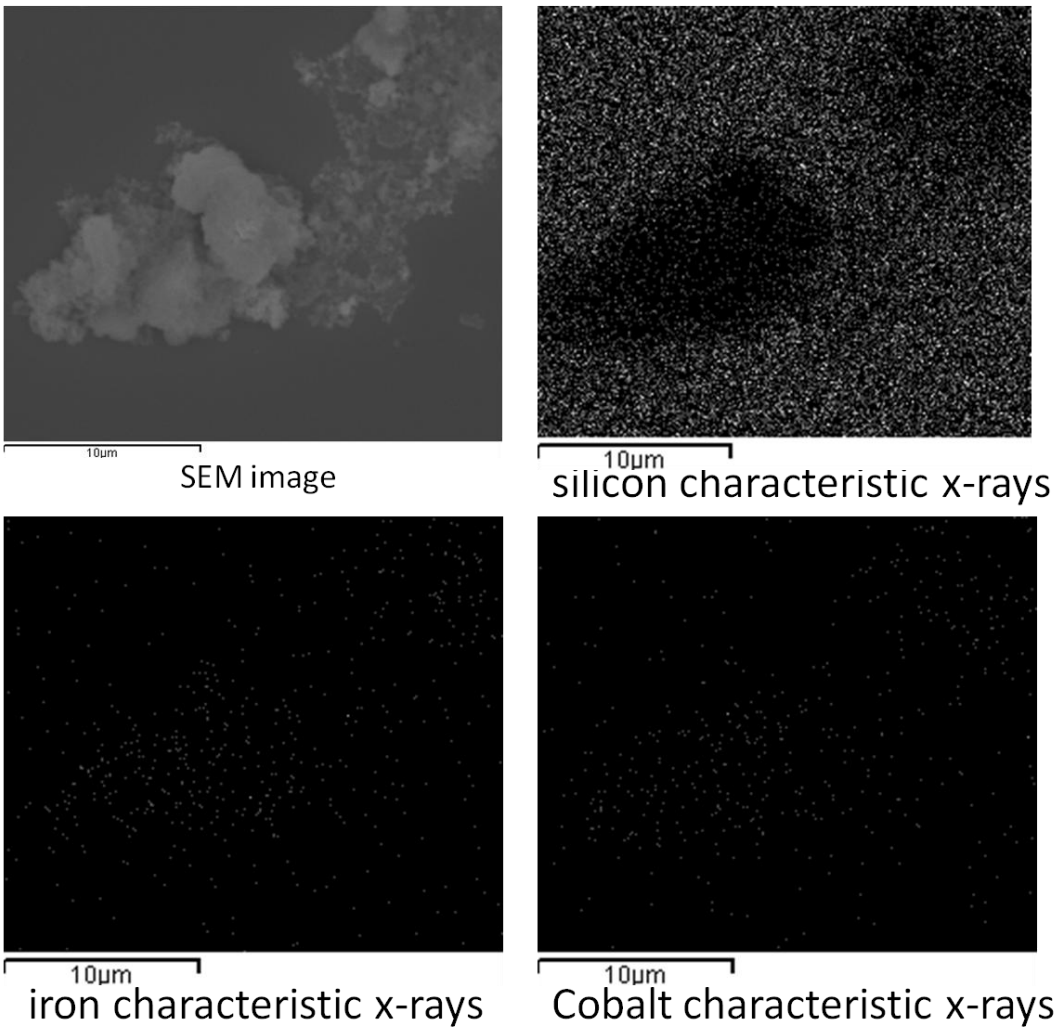

Figure 16: EDX analysis of FeCo nanoparticles.

One can see in the upper right image that the silicon background is obscured by the presence of the nanoparticle aggregates and that the iron and cobalt x-rays originate from the region which the nanoparticle aggregates are located. The Spectrum for these EDX images is shown below.

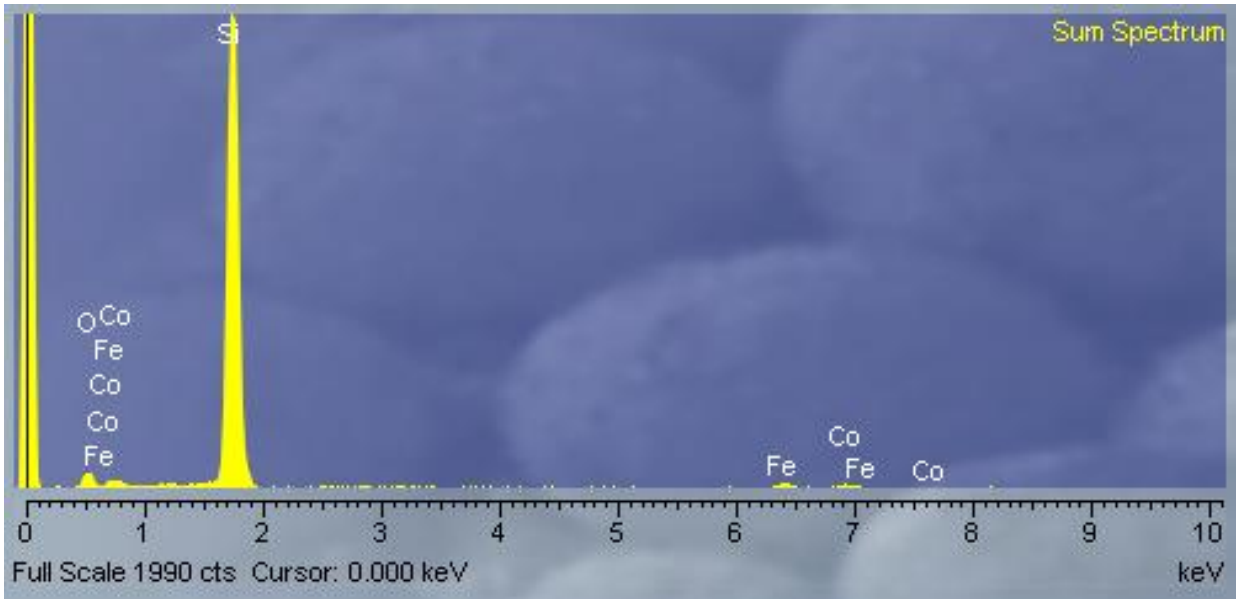

Figure 17: EDX spectrum for FeCo nanoparticles.

The spectrum clearly shows the presence of the iron and cobalt confirming the composition of the nanoparticles.

In the interest of fully characterizing these particles which we would be imaging, we also investigated the magnetic properties of the sample. The magnetization vs. applied field at room temperature for these particles was completed by Michael McHenry's group at CMU and is shown below.

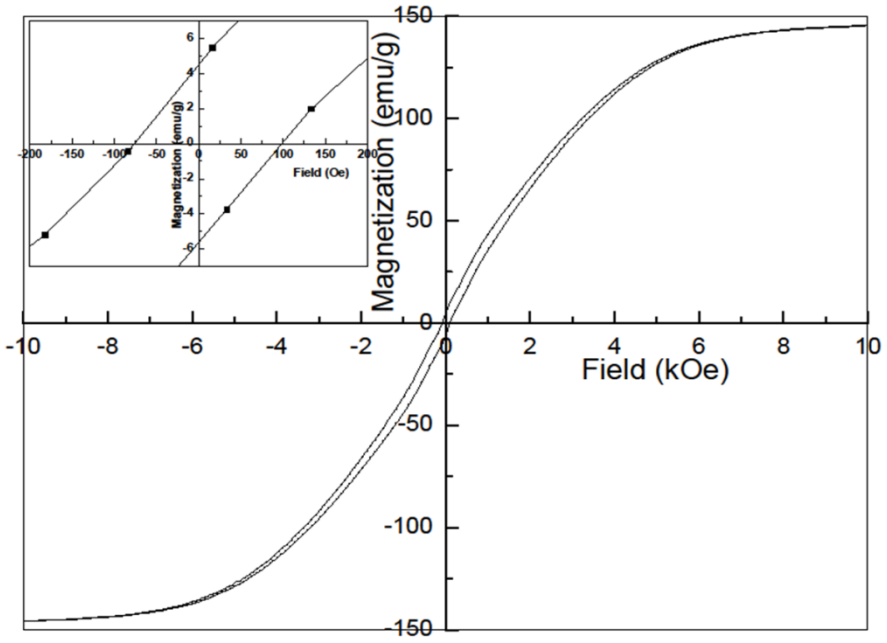

Figure 18: M-H plot at room temperature for the FeCo nanoparticles.

From the M-H data, we see that the FeCo nanoparticles are ferromagnetic with a coercivity of 100G. Therefore, in order to reverse the magnetization, the magnetic field stage must be able to apply at least 100G at the samples location. As shown previously, the electromagnet which is closer to the sample on the stage that I designed can produce 130G at the sample at 1Aand therefore we conducted the experiment using only that magnet.

5. Experimental Procedure

Once samples have been prepared as described above, the samples first have to be tested for appropriate uniformity of nanoparticle dispersion. This is accomplished by imaging the samples first with a scanning electron microscope and conventional atomic force microscopy. Once we have verified that the magnetic nanoparticles are uniformly dispersed, they can be imaged with magnetic force microscopy. As mentioned earlier, magnetic force microscopy requires a magnetic probe. For this experiment, magnetic probes from NT-MDT were used which were antimony doped single crystal silicon cantilevers with a 40 nm Cobalt/Chromium magnetic coating.

Cantilever series	Cantilever length, L±5μm	Cantilever width, W±3μm	Cantilever thickness, T±0.5 μm	Resonant frequency, kHz			Force constant, N/m		
				min	typical	max	min	typical	max
FMG01	225	32	2.5	50	60	70	1	3	5

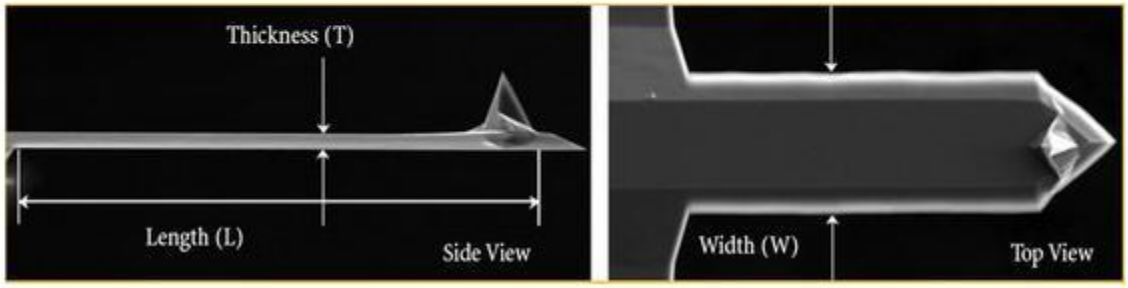

Figure 19: FMG01 cantilevers from NT-MDT

The cantilevers were magnetized prior to using them and a hard drive was imaged to ensure that they were properly able to detect a magnetic signal. Once an appropriate position on the sample was chosen, the magnetic nanoparticles were then imaged with atomic and magnetic force microscopy which records the particle height and cantilever phase respectively. Then, using the magnetic field stage, a field of 130 gauss was applied to the nanoparticles and the AFM/MFM height and phase were again

recorded. The current direction through the electromagnets was then reversed, reversing the applied magnetic field, and the AFM/MFM signal was again recorded.

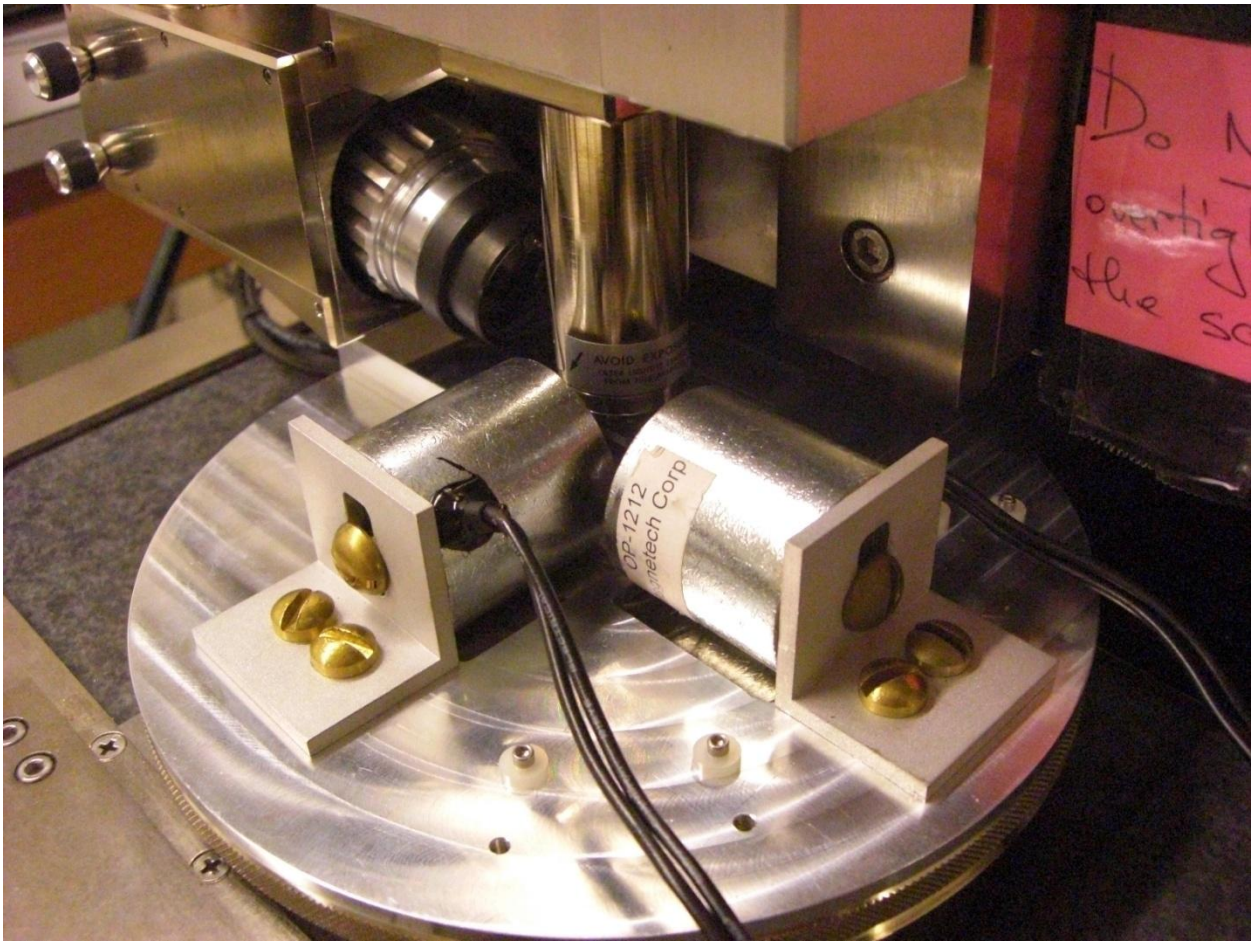

Figure 20: Magnetic field stage with Veeco Dimension 3000 AFM/MFM

In order to understand how the magnetic fields affected the imaging capabilities of the microscope, a calibration grating was imaged using the same procedure. The calibration grating is non-magnetic, so any changes that occurred as a result of the applied magnetic field had to be taken into consideration when I analyzed the results of the nanoparticle imaging.

6. Discussion and results

6.1 Calibration grating imaging

The imaging of the calibration grating demonstrates that the applied magnetic field causes distortion in the AFM/MFM image unrelated to magnetic contrast in the sample. When the field is applied to the microscope, there is an apparent drift of the sample or tip which causes the image to be distorted, as is shown in a comparison of figures 21 and 22. Figures 21-25 are a series of images taken without changing the scan location and are taken sequentially after the noted periods of time.

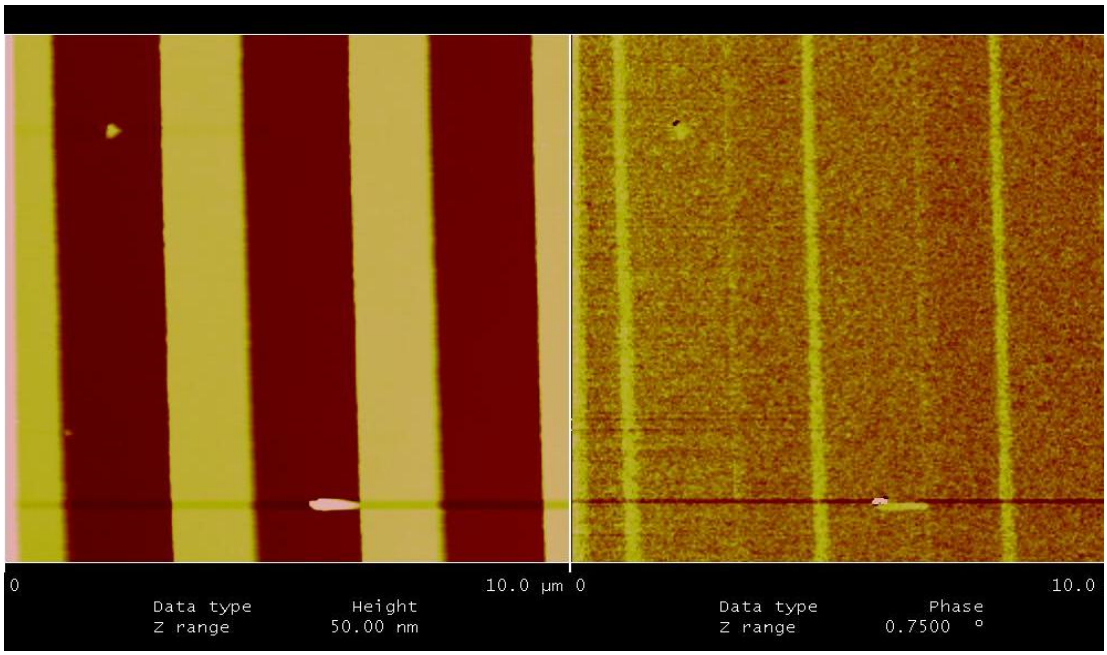

Figure 21: AFM/MFM image of a calibration grating with no applied field.

Figure 21 shows the calibration grating with the height of the sample mapped on the left and the cantilever phase change, normally the magnetic signal, on the right. While the calibration grating is composed of silicon and is not magnetic, some phase signal is evident. This effect is likely the result of

the cantilever being driven only 10 nm from the surface of the sample, where it is affected by surface interactions such as the Van der Waals force.

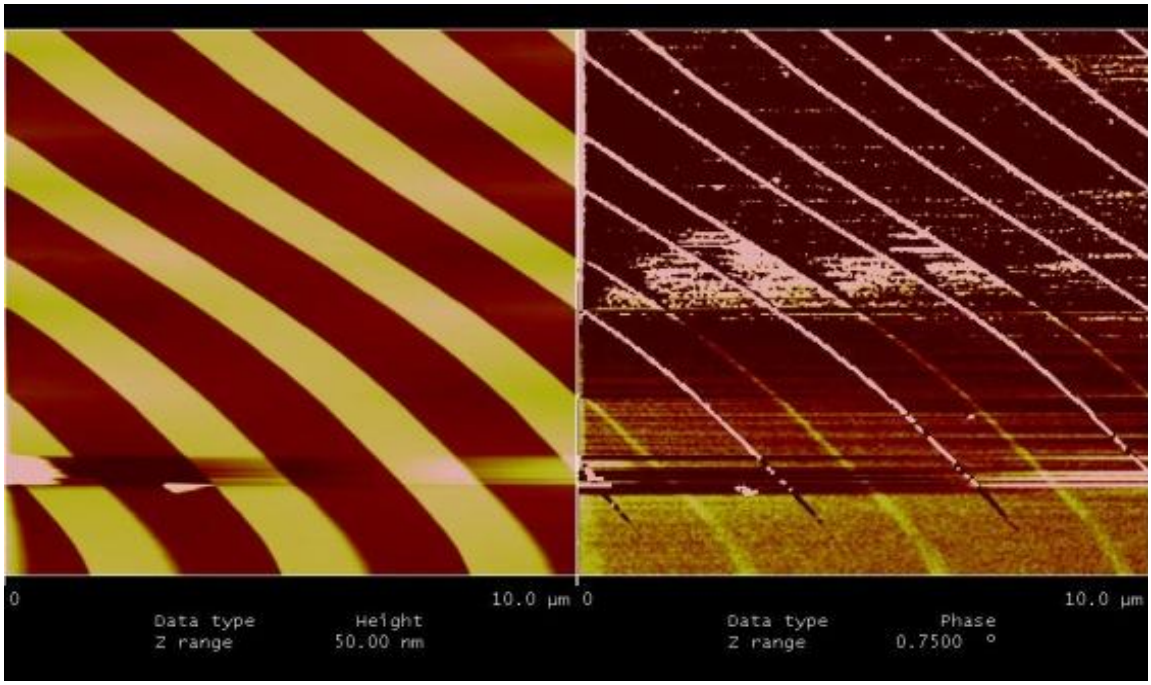

Figure 22: AFM/MFM image of calibration grating with 130 gauss field immediately after turning on the field. Scan direction is up.

Figure 22 was recorded after finishing the scan for figure 21 and shows us that once the field is turned on, the calibration lines are distorted, indicating that there is a force or movement of the sample (or of the cantilever tip or scan head) to the left, perpendicular to the applied magnetic field. The cantilever scans across the sample and moves up or down one line at a time depending on the direction of the scan. In the above image, the scan direction is upwards. The distortion of the calibration lines to the left therefore indicates a force to or movement to the left, perpendicular to the applied magnetic field.

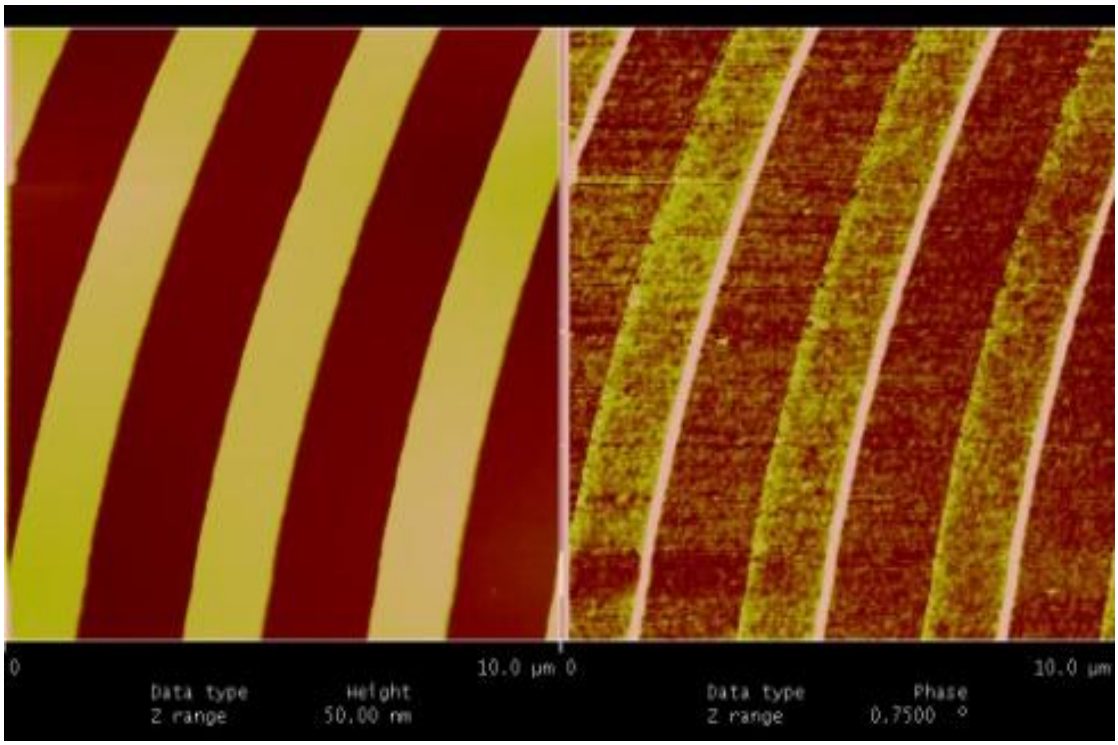

Figure 23: AFM/MFM image of calibration grating with 130 gauss field 30 minutes after turning on the field. Scan direction is down.

The Image In figure 23 was recorded 30 minutes after figure 21 and one can see that the apparent direction of the force or shift is to the right. However, the scan direction has been reversed and the cantilever is now scanning towards the bottom of the page. This also suggests a force or shift to the left. Also, the magnitude of the distortion is decreased after 30 minutes of constant applied field.

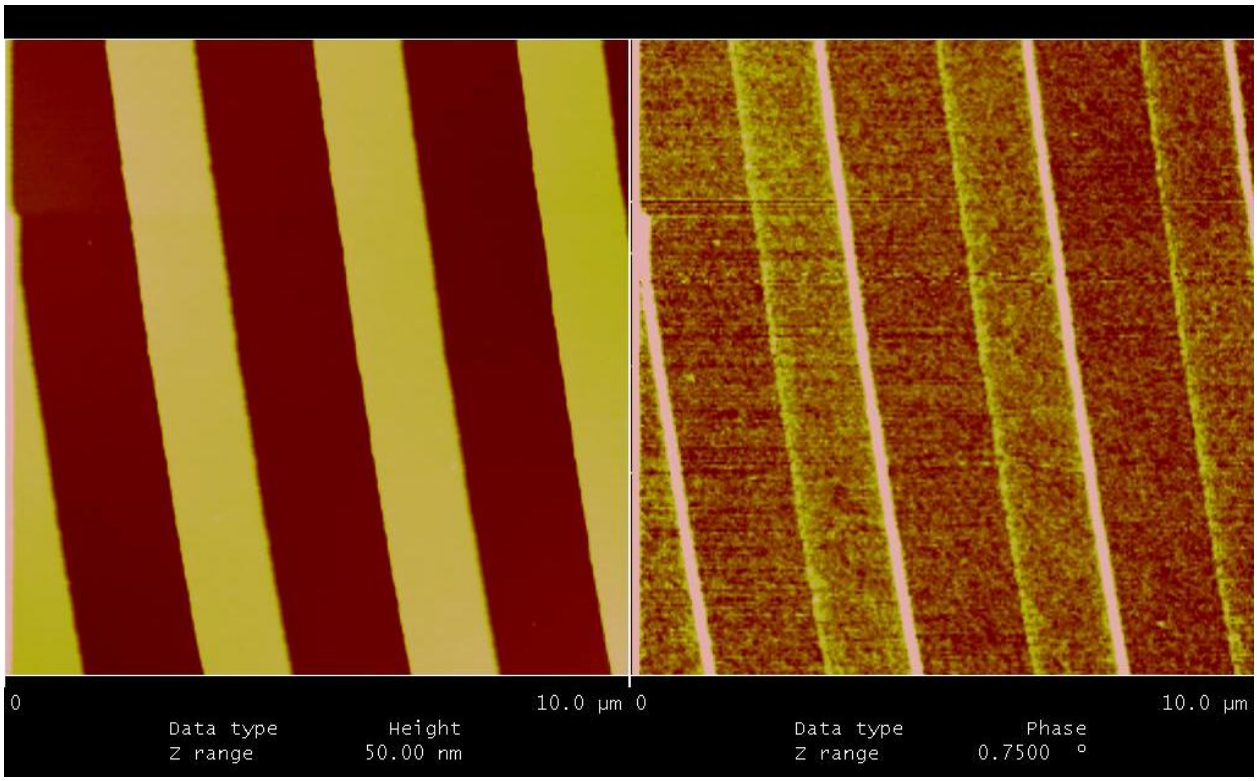

Figure 24: AFM/MFM image of calibration grating with 130 gauss field 60 minutes after turning on the field. Scan direction is up.

In figure 24, the scan direction is up once again and the distortion follows the same pattern as figure 23. However, the magnitude of the distortion is reduced after a constantly applied field for 60 minutes. The behavior of this distortion is that it decreases to some constant value over time. Usually within 1 hour the distortion is constant. This suggests that whatever is causing the distortion is saturating.

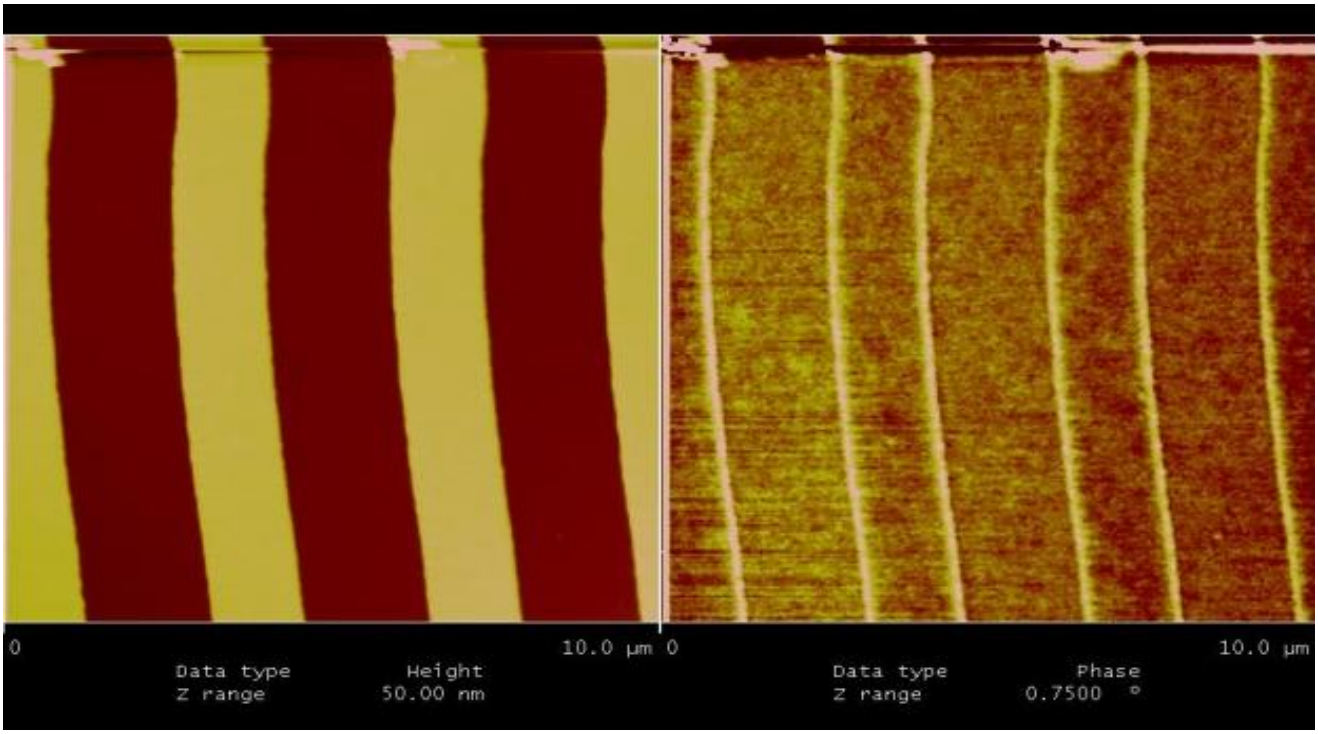

Figure 25: AFM/MFM image of calibration grating with 75 minutes after initially turning on the field. This image was acquired immediately after turning off the field. Scan direction is up.

Once the field is turned off, the image slowly relaxes back to its original state. The scan direction in figure 25 is up, so at the bottom of the scan, the lines are more distorted and, as time passes, they begin to straighten out. This reflects the difference between the image with applied field and the image with no applied field. In the bottom of the image, the scan lines remain distorted similarly to figure 24. In the top of the image the scan lines straighten out similarly to the initial scan, figure 22, without applied field.

There are two possibilities for the cause of the distortion. The first possible cause is that the electromagnet is applying a force to the scanner. We have determined that the scanner consists of a steel sheath covering a piezo tube. Therefore, it could feel a force from the electromagnet and cause the shifts that are seen in these images. This would also explain the saturating behavior because eventually, scanner motion will become limited by the surrounding hardware.

The second potential source of the distortion is the heat which is given off by the electromagnet. The electromagnet has a relatively high resistance, around 8-12 ohms depending on the temperature, and we are applying a current of 1 A. 60 watts of power is being generated, and as a result, a lot of heat was coming off the magnet. Since the entire stage is constructed of aluminum, the stage could be expanding underneath the sample causing a local movement of the sample. The shifts seen for the calibration grating are of the order of a micron and therefore a large temperature gradient is not necessary in order to attain these expansions. The expression for linear expansion is given by:

$$\frac{\Delta L}{L} = \alpha \Delta T \tag{18}$$

where L is the length of the stage, T is the temperature, and α is the linear expansion coefficient. Using the linear expansion coefficient for aluminum, and assuming a one micron expansion, the required temperature change is:

$$\frac{1 \times 10^{-6} m}{.1 m} \frac{1}{23 \times 10^{-6} / ^{\circ} c} = \Delta T = .43 \, ^{\circ} c \tag{19}$$

It is reasonable to assume that the surrounding AFM components (such as the stage) and sample could experience a temperature change on the order of a half a degree Celsius as a result of such extreme amounts of heat being generated by the electromagnet.

6.2 Magnetic Signals From Nanoparticles

I first imaged the magnetic nanoparticles without applying any external magnetic field. The results are shown below.

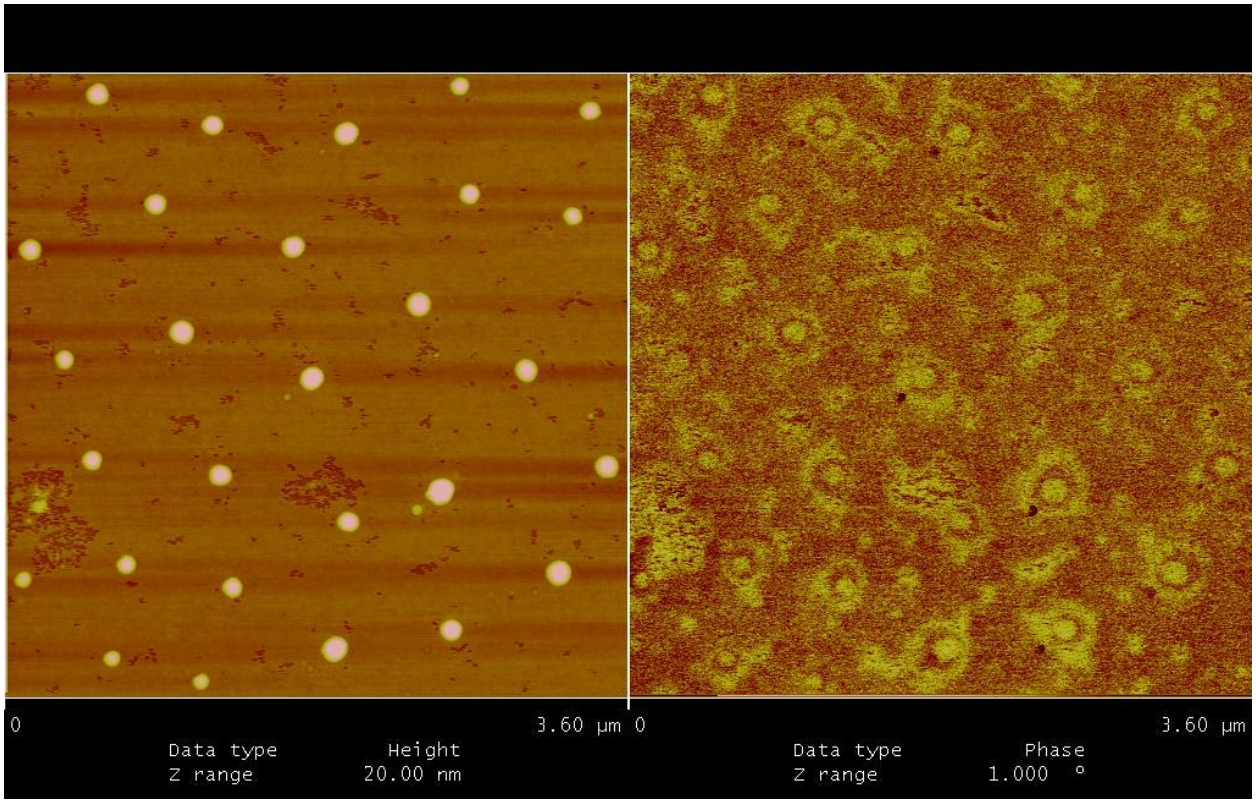

Figure 26: AFM particle height (left) and MFM signal (right) of FeCo nanoparticles on silicon without externally applied field.

The MFM signal in figure 26 shows a round phase signal centered at the location of the particle and a surrounding ring. In order to understand this behavior and interpret it as a magnetic signature I developed simulations using Matlab to model the interaction of a magnetic tip with the magnetic nanoparticles. In this case, it appears that the particles' and the tip's magnetizations are aligned along the z-axis or out of plane. For this simulation I assumed that the particle and the tip were each dipole

point particles with out of plane magnetization along the z-direction. The results of this simulation are shown below.

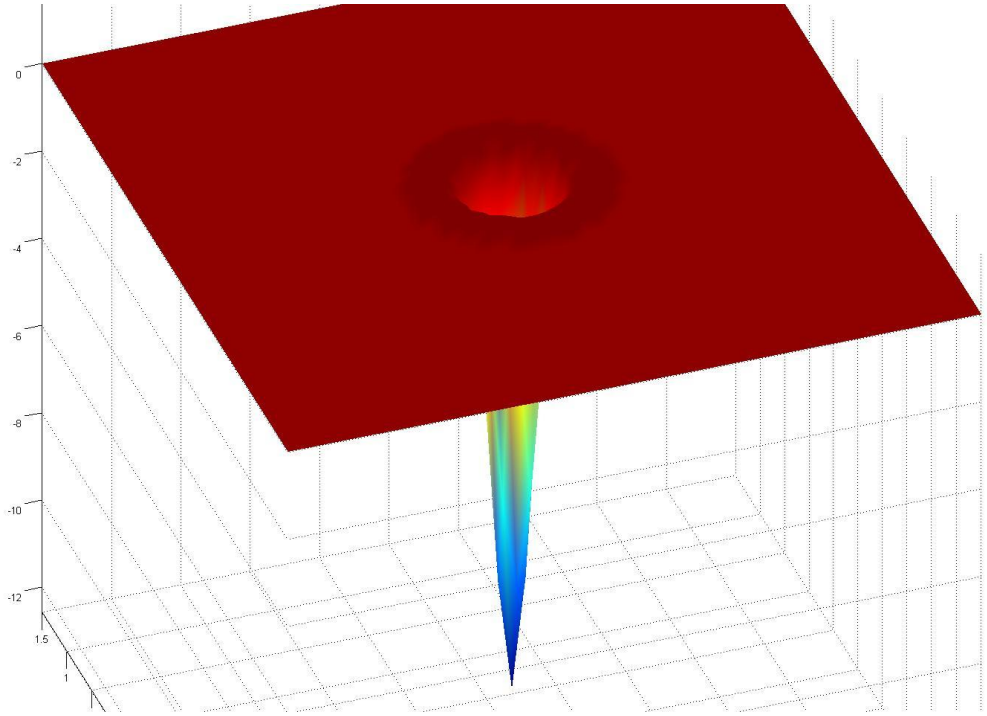

Figure 27: Simulated MFM signal from point particle dipole with out of plane magnetization.

This simulation shows the signal that the microscope would obtain from an ideal point particle dipole aligned out of plane and parallel to the tip's magnetization. As the microscope detects a shift in frequency of the cantilever, this simulation shows the gradient of the magnetic force as discussed earlier. The notable feature of this model is that the signal is centered at the location of the particle with a ring of opposite force gradient around the center. A single line from this image is shown below.

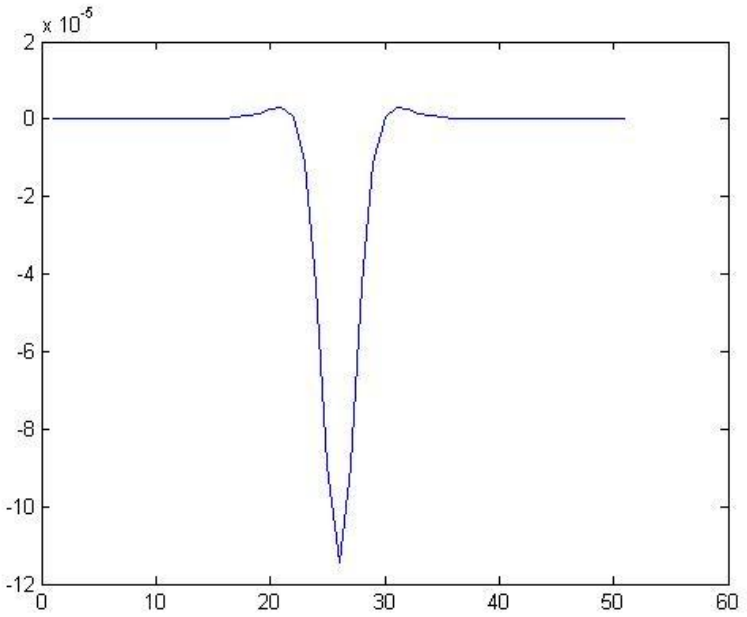

Figure 28: A single line from figure 27.

While the simulated model does not match exactly to the measurements, the ring present in both images suggests that the signal is magnetic. The reason for the poor agreement is that the actual system is much more complicated and consists of extended objects. In order to create an accurate model of the physical system, I needed to know the geometry and volume of the magnetic material on the cantilever. I determined this by using a Focused Ion Beam to image and cut cross sections of the cantilever. The cross sectioned cantilever is shown in figure 29.

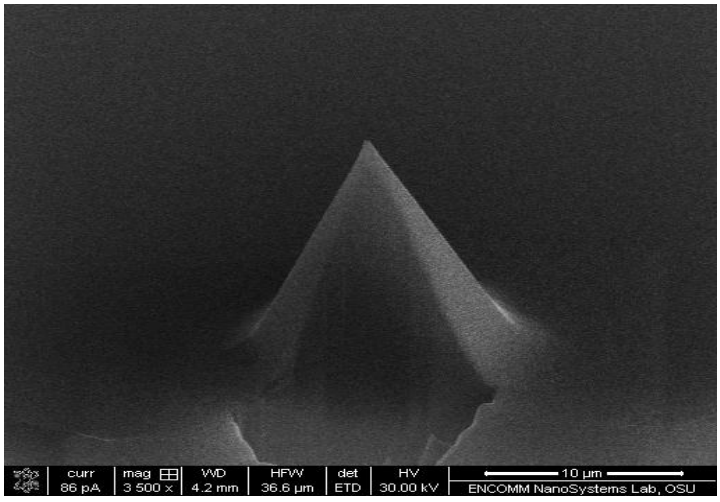

Figure 29: Focused Ion Beam cross sectioned MFM cantilever.

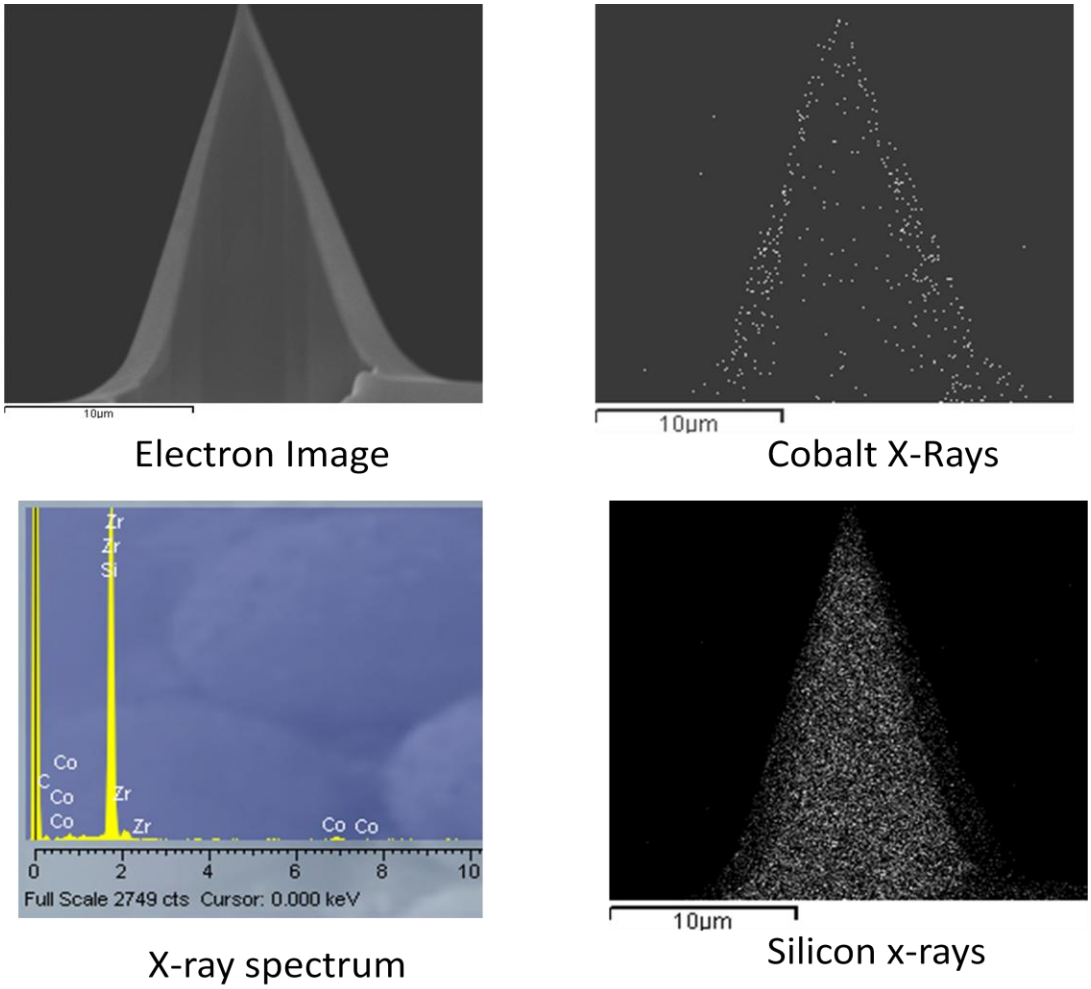

Figure 30: EDX images of cross sectioned MFM cantilever.

By analyzing the EDX images, I determined that the magnetic coating of the cantilever varies from around 100 nm thick at the tip to almost 1000 nm thick at the base. This larger volume of magnetic material coating the conical tip creates a complex geometry which is difficult to model. Therefore, it is not clear whether the signatures shown in figure 26 are the expected magnetic behavior for this interacting system. Next, I will show result from the nanoparticles imaged with external magnetic fields as outlined in the experimental procedure.

While there are distortions caused by applying the external magnetic field that are not necessarily related to any magnetic signal, after waiting one hour, the distortions are smaller and remain constant. Therefore, I can image the magnetic nanoparticles with the experimental procedure previously outlined.

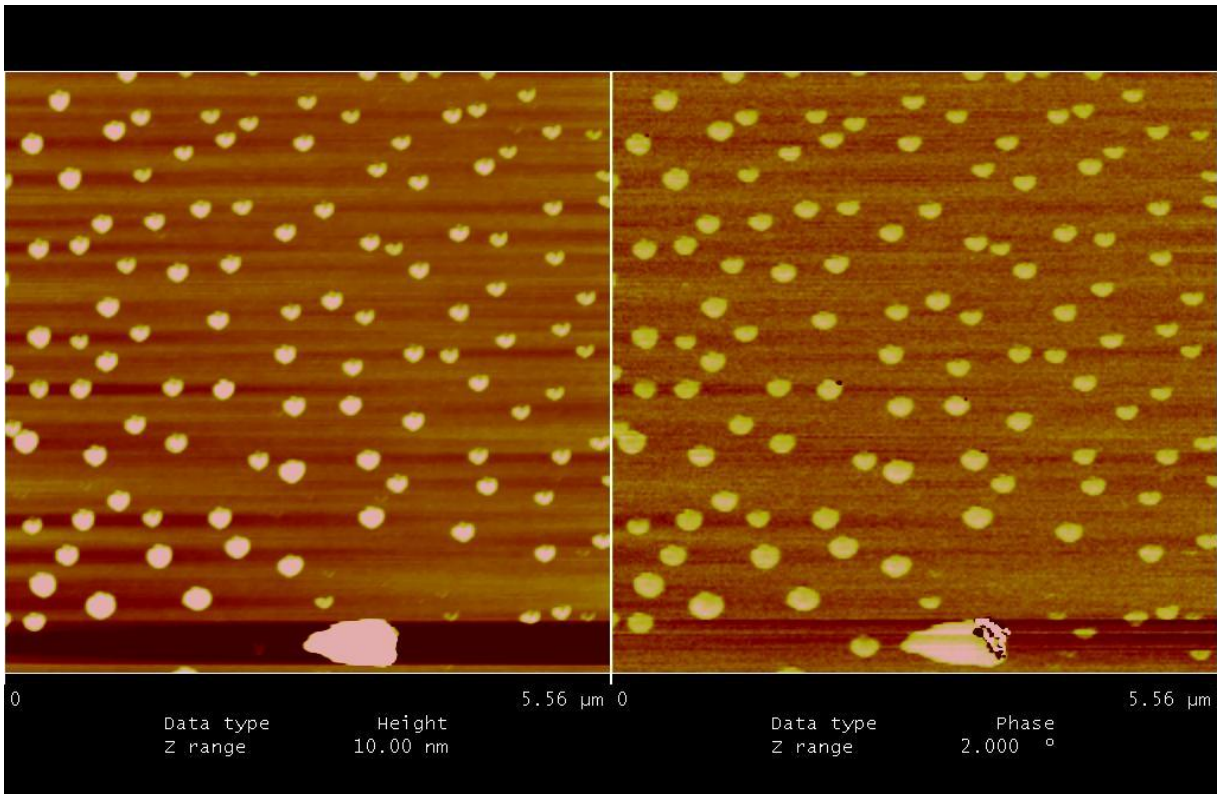

Figure 31: AFM/MFM image of FeCo nanoparticles without an applied magnetic field. Tip sample separation is 20 nm.

In this image, there is no magnetic field and the MFM signal shows only round signatures for the magnetic nanoparticles. Once the magnetic field is turned on and 1 hour has passed, the nanoparticles show a dipolar phase pattern, shown in figure 32. The dipolar phase pattern is evident by the change from light to dark from the bottom to the top of the particles indicating the tip moving over attractive and repulsive regimes indicative of a magnetic dipole. The direction of the magnetic field is from the bottom to the top of the image and this is the direction of the aligned dipoles.

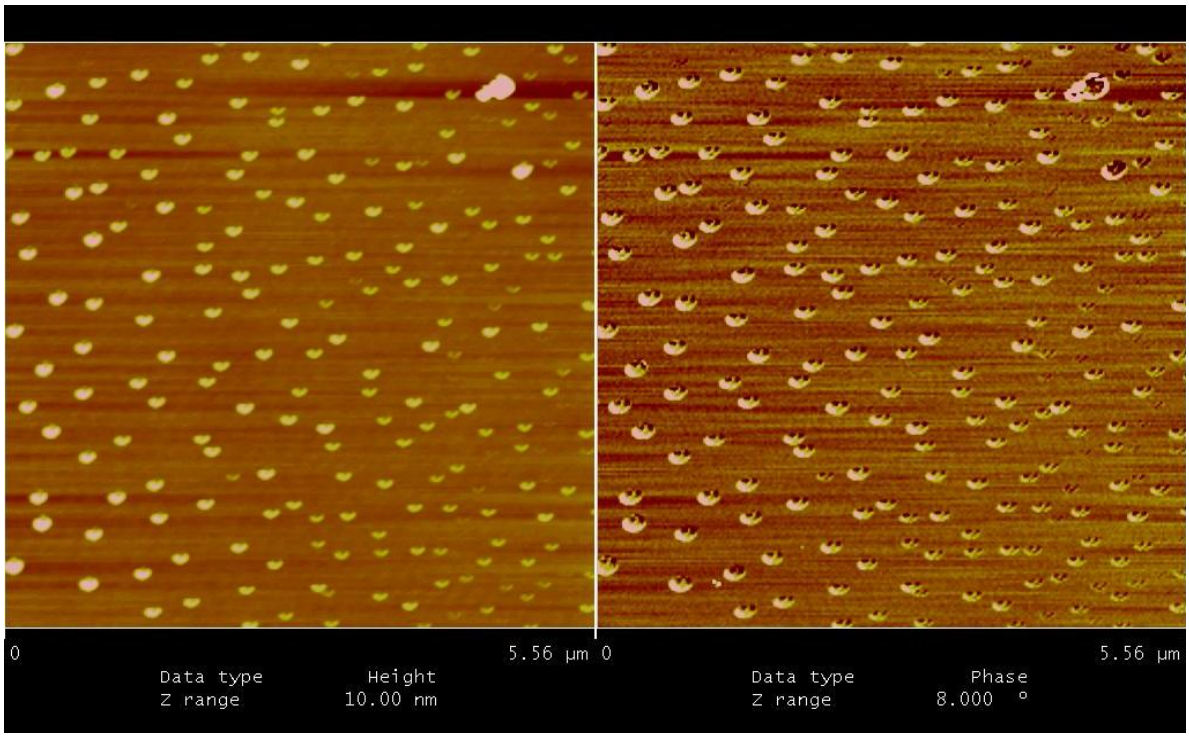

Figure 32: AFM/MFM image of FeCo nanoparticles with an applied magnetic field. Tip sample separation is 20 nm.

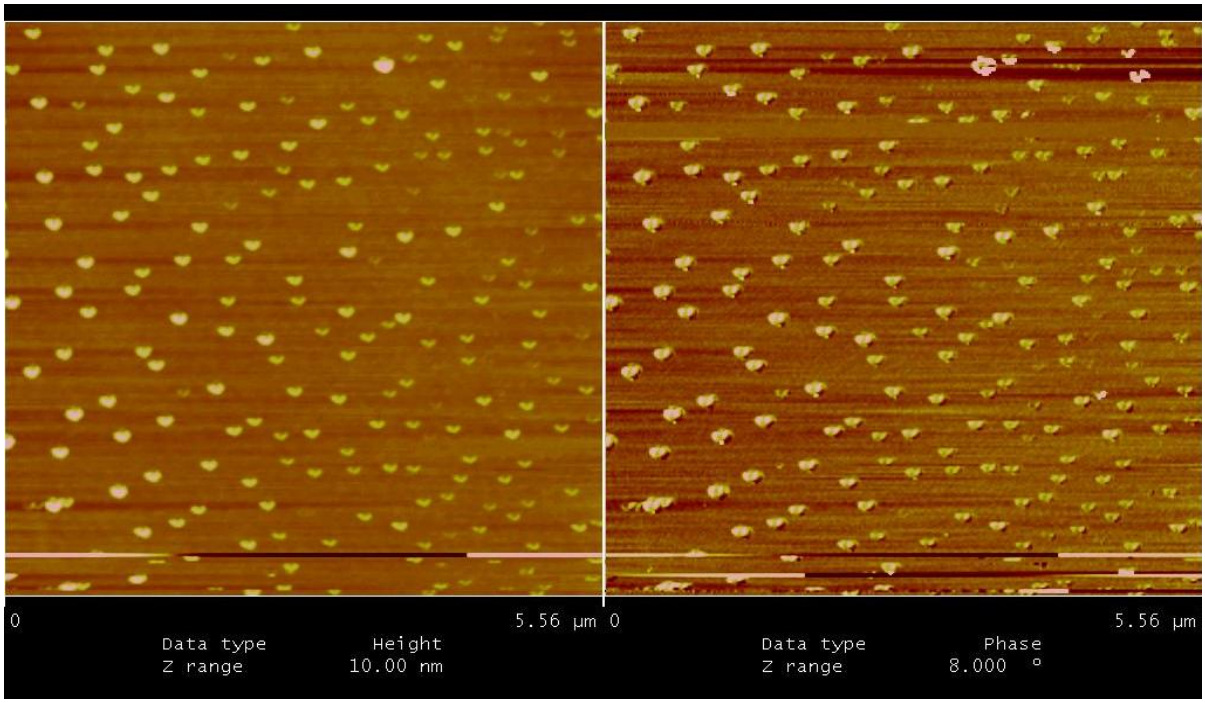

Figure 33: AFM/MFM image of FeCo nanoparticles with an applied magnetic field in the opposite direction as in Figure 28. Tip sample separation is 20 nm.

In figure 33, the current of the electromagnet is reversed relative to figure 32. When the current is reversed, the direction of the dipoles is reversed as shown by the negative portion of the phase moving from the top of the particles to the bottom of the particles. In order to understand the behavior in these images, I will once again turn to Matlab simulations. In this case, since we are applying a magnetic field in plane, the particles magnetization will be in plane. Using the same approximations as before but now modeling the tips interaction with a particle having an in plane magnetization, the simulations demonstrate a dipolar pattern. This simulation shows a similar change from positive to negative force gradient as the probe scans in the direction of the particle's magnetization. Showing a single line scan from figure 32, we can see similar behavior. If the magnetization is reversed as we have done in the actual measurements, the simulations also show that the positive and negative force gradients switch.

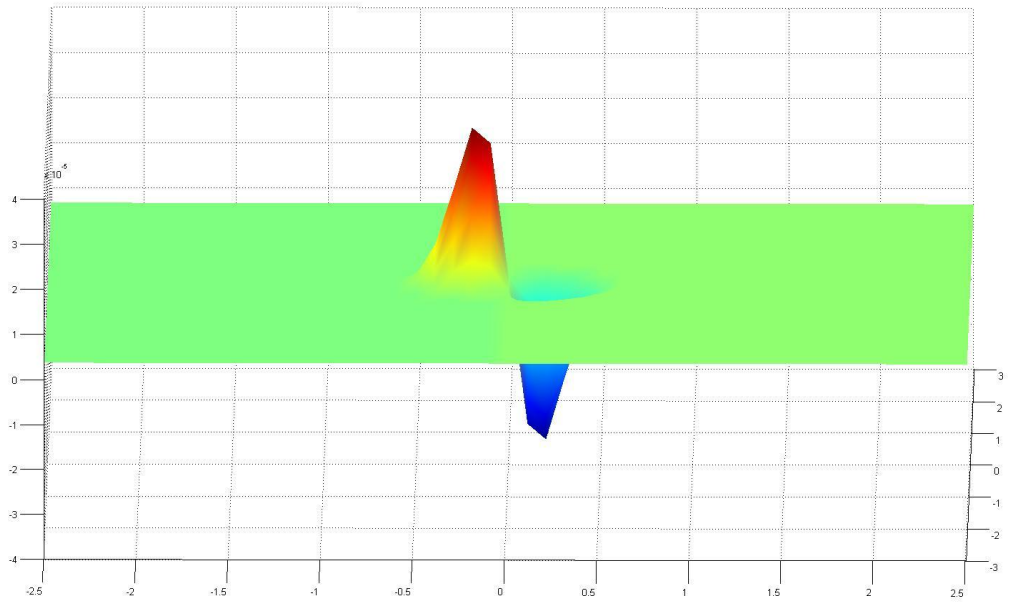

Figure 34: Simulated MFM signal from a point particle dipole with in plane magnetization.

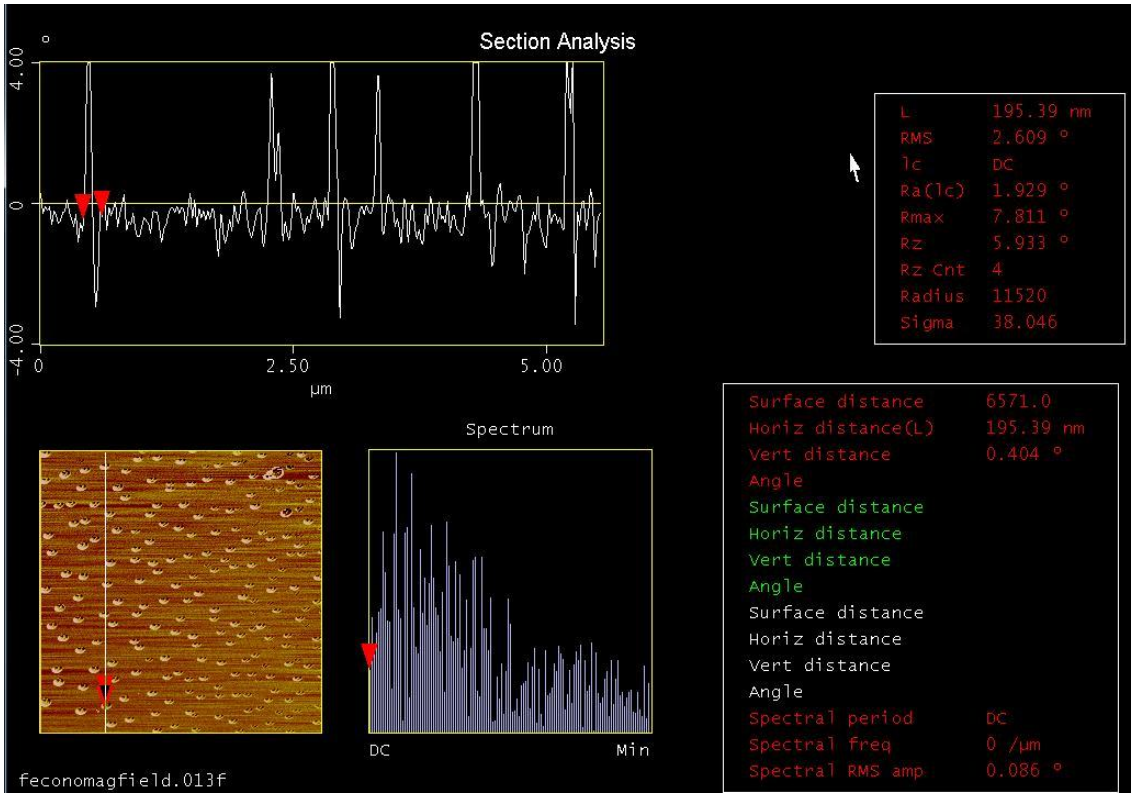

Figure 35: Single line scan from figure 32.

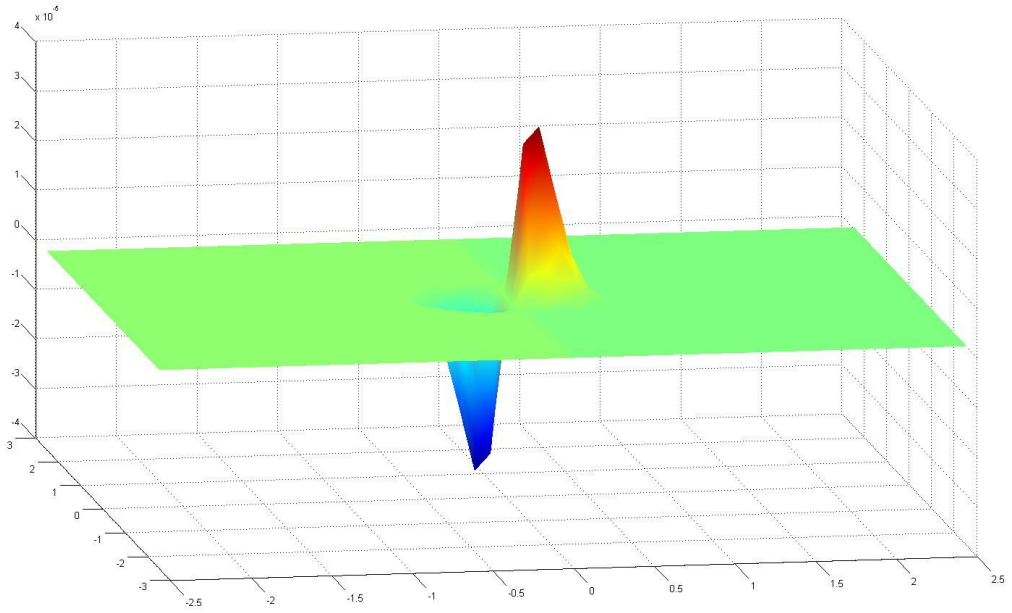

Figure 36: Simulated MFM signal from point particle dipole with opposite in plane magnetization.

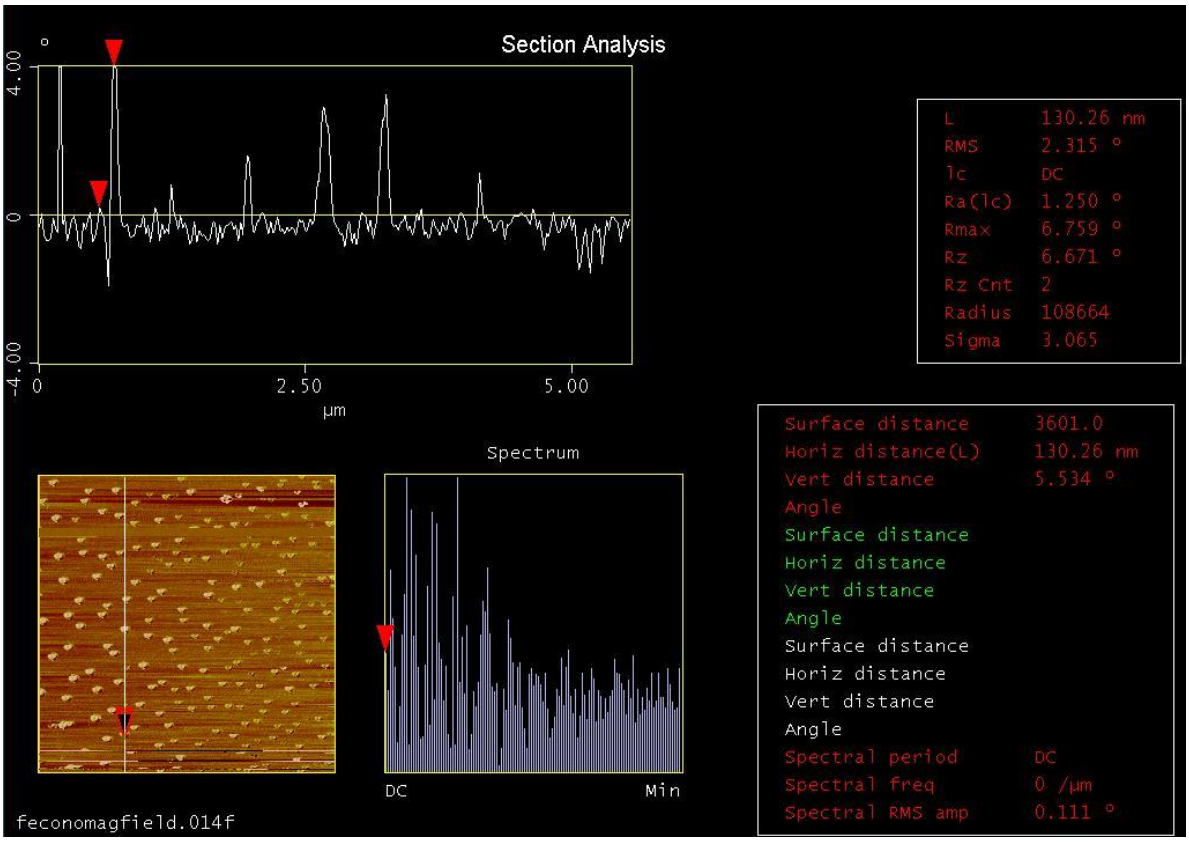

Figure 37: Single line scan from figure 33.

While the single line scans fit well with the simulations, one issue with the above results is that there is some distortion to the image. In figures 32 and 33, the particles are not as round as they should be compared to figure 31. A likely explanation for the distortions in the shape of the particle is that the magnetized tip attracts the nanoparticles and during the course of scanning on such nanoparticle got stuck to the tip. The particle stuck to the tip would create a double tip and therefore every particle would interact with both the cantilever tip and the particles stuck to the tip. This would make the tip larger and therefore it would not be as effective in resolving the shape of the nanoparticles. This additional effect complicates the simulations and therefore it is difficult to match the theory closely to the measured results.

7. Conclusion

The primary component of this thesis project was to develop magnetic force microscopy techniques for imaging magnetic nanoparticles. However, there were additional considerations which I had to address in order to achieve this goal. The first aspect was developing a technique to uniformly disperse the nanoparticles onto a substrate. I have shown that the method described in this thesis produces excellent results. The next consideration was to design a stage which could apply variable external magnetic fields in conjunction with MFM. The results are shown in this thesis are successful but limited by the distortions caused by the stage. I have considered an improved stage design which may be implemented in the future. The improved stage would eliminate the large magnetic force on the scanner and reduce the heating near the sample location. The improved design consists of an electromagnet which is farther away from the sample location to reduce the heating. The electromagnet sits in the center of two curved pieces of iron which have ends close to the sample and become magnetized by the electromagnet creating a field at the samples location. The ends of the pieces of iron can be narrow so that they only produce a field near the sample and not along the length of the scanner, thus reducing the magnetic force affecting the scanner.

The images of magnetic particles show some magnetic behavior which can be modeled using programs. However, the ability to precisely model the interactions is limited by the complex geometries present in the particles themselves as well as the tip of the cantilever. In order to simplify quantitative analysis of the interactions, a new type of MFM cantilever could be used. Our collaborators at the Leibniz Institute for Solid State and Materials Research are developing a new MFM cantilever which uses an iron filled carbon nanotube attached to the end of a silicon cantilever rather than a silicon cantilever coated with magnetic material. The Iron filled carbon nanotube has

an extremely high aspect ratio and would therefore behave like a magnetic monopole near the end of the tube.

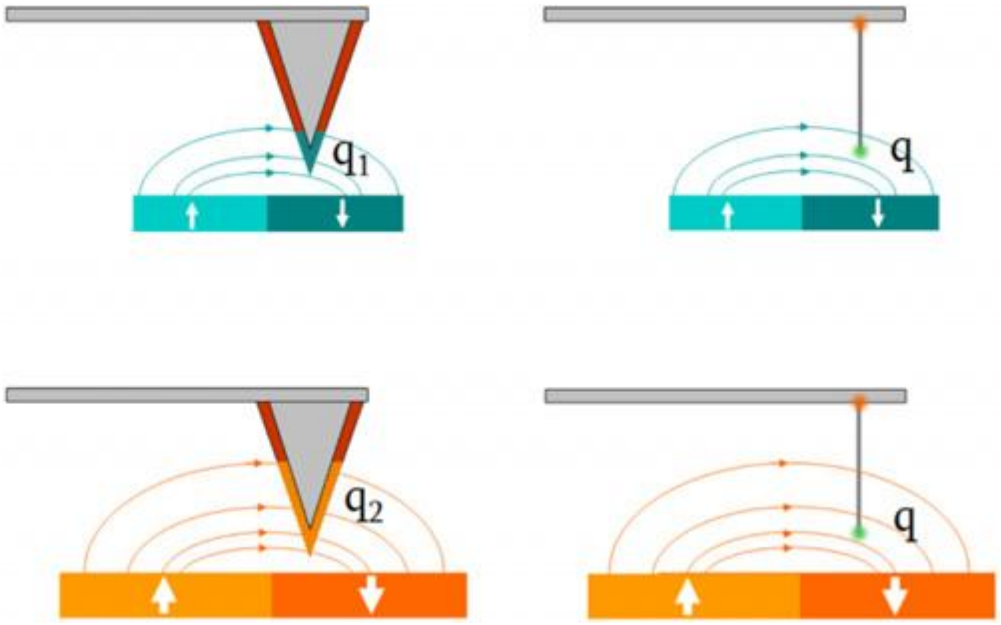

Figure 38: Depending on the sample stray field geometry, different volumes of the magnetic coating of a conventional probe are involved in the imaging process, leading to different values of the effective probe monopole moment *q* (left). In the case of a rod-shaped magnetic dipole much longer than the stray field's decay length, only the lower monopole takes part in the interaction (right) [27]

This would increase the sensitivity of the MFM cantilever as well as simplify any geometry present in calculating the force on the MFM cantilever. While there are still many challenges to be addressed in order to fully understand magnetic signals from nanoparticles, the work completed for this thesis project develops many of the required techniques for the ultimate goal of quantitative MFM. In addition, the images collected can be simulated using simple magnetic models and agree relatively well with the theory.

8. Acknowledgements

This project represents the culmination of three years and three different projects while participating in undergraduate research at Ohio State. Even though I did not work with you all for this final project, I want to thank K.C. Fong for being a tough mentor and challenging me to learn what it means to be a physicist, and to Michael Herman for helping me to start my own project. In addition, I want to thank the entire Hammel Research group for making me feel like part of the family.

For help with this specific project, I have to thank Richelle Teeling for helping me through that rough first summer when no one knew anything about this project. It would have been a huge challenge to work alone when everything was so new. A special thanks goes out to Camelia Marginean and Denis Pelekhov for your expert help and advice. I could not have come as far as I did without your patience and expertise. I also want to thank our collaborators in Biomedical Engineering: Tanya Nocera and Professor Gunjan Agarwal. In addition, I have to thank Kris Dunlap for all of your help throughout the years. I am sure you were busy but you were always willing to help me with anything I asked of you.

Last and most importantly, thank you Professor Hammel. My greatest accomplishments and pride in myself are all because of you. A large part of how I define myself and my confidience in my ability to succeed in an ever more competitive world is the result of what I learned while working in your group. I truly would not be the same person without what I learned from you. I can never thank you enough for the priceless gift you have given me and what I learned from you will always be part of who I am. Also, I had so much fun while learning from you and your group members that my college education would not have been the same without the great times I had while being part of

your group. Thank you for showing confidence in me and allowing me to learn from your exceptional group.

9. Bibliography

[1] H.Zhang, L. R. Moore, M.Zborowsk i, P. S. Williams, S. Margel, J.J. Chalmers, Analyst 2005, 130, 514–527.

[2] B.Sc hmitz, A.Radbruc h, T.Kum mel, C. Wickenhauser, H.Korb , M.L. Hansmann, J. Thiele, R. Fischer, Eur.J. Haematol. 1994, 52, 267–275.

[3] S.Miltenyi, W.Muller , W. Weichel, A.Radbruc h, Cytometry 1990, 11, 231–238.

[4] M.Savoiard o, F. Girotti, L.Strada, E. Ciceri, J.Neur al Transm. Suppl. 1994, 42, 93–110.

[5] A.Bizzi, R. A.Brooks, A.Brunetti, J. M.Hill, J. R.Alger , R. S. Miletich, T.L. Francavilla, G. Di Chiro, Radiology 1990, 177, 59–65.

[6] X. Huang, R.D . Moir, R.E. Tanzi, A.L. Bush, J. T. Rogers, Ann. N.Y. Acad. Sci. 2004, 1012, 153–163.

[7] L.Y. Chau, Proc.Natl. Sci. Counc. Repub. China B 2000, 24, 151–155.

[8] R.B. Frankel, Annu.Rev. Biophys.Bioeng. 1984, 13, 85–103.

[9] D. G.Ramlan, S. J. May, J. G.Zheng, J. E.Allen, B.W. Wessels, L.J. Lauhon, Nano Lett. 2006, 6, 50–54.

[10] Y. Takamura, R. V. Chopdekar, A.Sc holl, A.Doran, J. A.Liddle, B. Harteneck, Y.Suzuki, Nano Lett. 2006, 6, 1287–1291.

[11] M.Ras a, A. P.Philips e, J.Magn.Magn.Mater . 2002, 252, 101–103.

[12] J.Dobson, FEBS Lett. 2001, 496, 1–5.

[13] C.E. Diebel, R. Proksch, C.R. Green, P. Neilson, M.M. Walker, Nature 2000, 406, 299–302.

[14] A.L. Martinelli, A.B. Filho, R.F . Franco, M.H. Tavella, L.N. Ramalho, S.Zuc oloto, S. S.Rodrigues, M. A.Zag o, J Gastroenterol. Hepatol. 2004, 19, 1036–1041.

[15] Y.Amemiya, T. Tanaka, B. Yoza, T.Matsuna ga, J.Biotechnol. 2005, 120, 308–314.

[16] M.Ras a, B.W.Ku ipers, A. P.Philips e, J.Coll oid Interface Sci. 2002, 250, 303–315.

[17] H.Shen, D.Long, L.Zhu, X.Li, Y.Dong, N.Jia, H.Zhou, X.Xin, Y. Sun, Biophys.Chem. 2006, 122, 1–4.

[18] L. Abelmenn, Systems and Materials for Information Storage, University of Twente, July 2005

[19] L. Abelmenn, Systems and Materials for Information Storage, University of Twente, July 2005

[20] M.Hanzlik, C.Heuneman n, E. H.Rçtzler , M. Winklhofer, N.Petersen, G.Fleissner , BioMetals 2000,13, 325–331.

[21] M.M. Walker, J.L. Kirschvink. J.Exp.Biol. 1988, 140, 35–49.

[22] J.L. Kirschvink, K.A. Kobayashi, B. J. Woodford, Proc.Natl. Acad.Sci. USA 1992, 89, 7683–7987.

[23] A. Hendrych, R. Kubínek and A. V. Zhukov, Formatex. 2007, 805-811

[24] L. Abelmenn, Systems and Materials for Information Storage, University of Twente, July 2005

[25] A. Hendrych, R. Kubínek and A. V. Zhukov, Formatex. 2007, 805-811

[26] G. Goya, T. Berquo´, and F. Fonseca, Journal of Appled Physics. 2003, 94, 5

[27] F. Wolny, T. Muhl, U. Weissker, K. Lipert, J. Schumann, A. Leonardt, and B. Buchner, IOPscience 2010, Nanotechnology 21, 435501